INTRINSIC AND THERMAL STRESS MODELLING FOR THIN-FILM MULTILAYERS

PERKIN-ELMER CORPORATION
NORWALK, CONNECTICUT

DECEMBER 1976

UNCLASSIFIED

SECURITY CLASSIFICATION OF THIS PAGE (When Data Entered)

REPORT DOCUMENTATION PAGE		READ INSTRUCTIONS BEFORE COMPLETING FORM
1. REPORT NUMBER	2. GOVT ACCESSION NO.	3. RECIPIENT'S CATALOG NUMBER
4. TITLE (and Subtitle) INTRINSIC AND THERMAL STRESS MODELLING FOR THIN-FILM MULTILAYERS		5. TYPE OF REPORT & PERIOD COVERED Semiannual Technical Report May 1976 - December 1976
		6. PERFORMING ORG. REPORT NUMBER 13262
7. AUTHOR(s) A. M. Ledger R. C. Bastien		8. CONTRACT OR GRANT NUMBER(s) DAA25-76-C-0410
9. PERFORMING ORGANIZATION NAME AND ADDRESS The Perkin-Elmer Corporation Norwalk, Connecticut 06856		10. PROGRAM ELEMENT, PROJECT, TASK AREA & WORK UNIT NUMBERS ARPA Work Order No. 3220
11. CONTROLLING OFFICE NAME AND ADDRESS Defense Advanced Research Projects Agency 1400 Wilson Boulevard Arlington, Virginia 22209		12. REPORT DATE December 1976 13. NUMBER OF PAGES 51
14. MONITORING AGENCY NAME & ADDRESS(if different from Controlling Office)		15. SECURITY CLASS. (of this report) Unclassified 15a. DECLASSIFICATION/DOWNGRADING SCHEDULE

16. DISTRIBUTION STATEMENT (of this Report)

Distribution of this document is unlimited.

17. DISTRIBUTION STATEMENT (of the abstract entered in Block 20, if different from Report)

18. SUPPLEMENTARY NOTES

19. KEY WORDS (Continue on reverse side if necessary and identify by block number)

Antireflection Coatings
High-Power Lasers
Infrared
Interferometer
Potassium Chloride
Stress
Windows

20. ABSTRACT (Continue on reverse side if necessary and identify by block number)

The measurement of induced stresses and thermally induced stresses in thin-film multilayer coatings is being investigated using an interferometric technique. Stress data is to be incorporated into a model for the prediction of thermally induced failure mechanisms in antireflection coatings for KCl windows at 10.6μ.

DD FORM 1 JAN 73 1473 EDITION OF 1 NOV 65 IS OBSOLETE

UNCLASSIFIED

SECURITY CLASSIFICATION OF THIS PAGE (When Data Entered)

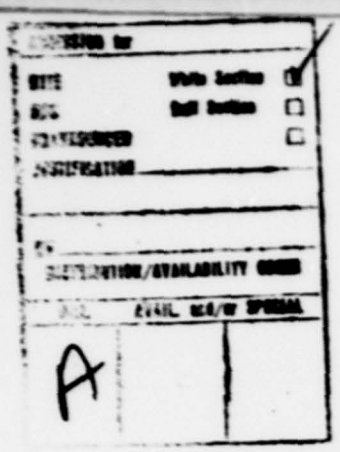

AD

INTRINSIC AND THERMAL STRESS MODELLING FOR THIN-FILM MULTILAYERS

SEMIANNUAL TECHNICAL REPORT

A. M. Ledger And R. C. Bastien
The Perkin-Elmer Corporation
Norwalk, Connecticut 06856

December 1976

Contract No. DAA25-76-C-0410

DEFENSE ADVANCED RESEARCH PROJECTS AGENCY
1400 WILSON BOULEVARD
ARLINGTON, VIRGINIA 22209

i (+)

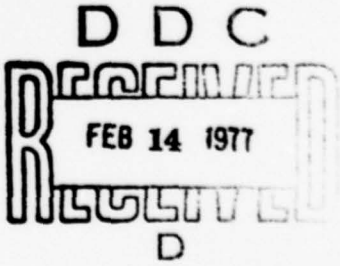

The findings in this report are not to be construed as an official Department of the Army position unless so designated by other authorized documents.

TABLE OF CONTENTS

LIST OF ILLUSTRATIONS

LIST OF ILLUSTRATIONS (Continued)

SECTION 1

INTRODUCTION

Multilayer dielectric coatings fabricated by thermal evaporation exist in a stressed condition due to intrinsic stress buildup during deposition, combined with temperature-induced stress changes established during post-deposition cooling. The resulting stress levels in multilayer coatings significantly influence the adhesive properties at the substrate/film or interfilm boundaries and affect the durability of the coating when exposed to severe environmental conditions.

Although stress levels in growing film structures have been measured and widely reported during recent decades, little progress has been made in establishing a quantitative link between induced stress and coating reliability for multilayer dielectric coatings. The present program has as its goal, therefore, the development of theoretical models to enable the thin-film designer to predict the durability of simple multilayer dielectric coatings, particularly antireflection coatings for high-expansion-coefficient laser windows such as polycrystalline potassium chloride. In order to limit the magnitude of such an investigation, we will be concerned with the durability of antireflection coatings consisting of 2 or 3 layers deposited onto potassium chloride and designed to give minimum reflectivity at 10.6 microns.

The program consists of the following subtasks to be completed during the present phase of the program

- Formulation of stress and reliability models
- Stress measurements of candidate materials
- Stress measurements of complete antireflection coatings
- Failure mechanism identification
- Evaluation of theoretical models
- Failure prediction under high-power laser irradiation

Work performed during the first six months of the program was concentrated in the following areas:

- Design, fabrication and testing of a system of stress-measuring interferometers to allow four simultaneous and independent stress measurements to be made during a single evaporation
- Literature search and a theoretical study to formulate stress addition models in thin-film multilayers

The stress-measuring interferometers, data recording system, and computer codes for data reduction were completed during December and are described in Section II. Theoretical studies completed to date aimed at generating computer models of stress addition, including thermal effects; these are described in Section III.

SECTION 2

STRESS MEASUREMENTS ON THIN FILMS

2.1 STRESS MEASUREMENT TECHNIQUES AND REQUIREMENTS

Stress measurements carried out during the growth or deposition phase of a thin film have been made by numerous authors and by many and differing techniques. The most common method in use is the measurement of the deflection of a thin glass beam or disc upon which the coating material is being deposited. Optical interference methods have been described by Hoffman[1] and Ennos[2], and displacement measurements by capacitative and electromechanical means have been reported by Campbell[3] and Hoffman[4]. Electron diffraction techniques reported by Halliday[5] and X-ray diffraction techniques by Kinabara[6] have also been used for thin-film stress measurements, but these methods are not as easily implemented as are the bending beam and disc techniques.

A comprehensive review of stress measurements and the mechanical properties of thin films has been given by Hoffman[7] and more recently by Kinosita[8] and Hoffman[9]. Stress studies have traditionally been carried out for metallic thin films to aid in explaining film nucleation and growth and only a few authors have investigated the stress properties of dielectric films. The two most comprehensive investigations of stress buildup in dielectric films have been made by Ennos[2], using laser interferometry, and Campbell [10],who utilized a capacitance measuring technique. Ennos measured the stress properties of ZnS, MgF_2, $THOF_2$, PbF_2, cryolite, chiolite, CaF_2, CaF_3, SiO, $PbCl_2$, TlCl, TlI, Ge, Te and CdTe during film deposition and investigated the effects of temperature, deposition rate and air exposure after deposition. The stress properties of alkali halide films has been reported by Campbell, who investigated LiF, NaF, NaCl, NaBr, KBr, and KI at various deposition rates.

Many of these materials can be used as the components in anti-reflection coatings for KCl windows for the 10-micron region; however, stress data was only obtained for mechanical film thicknesses up to the 2000Å range by Campbell and up to thicknesses of 5000Å by Ennos. Anti-reflection coatings of low-index materials for the 10-micron region require individual film thicknesses of 1.5 microns or more and ∿1 micron for high-index materials. Consequently, intrinsic stresses for "thick" films must be obtained during the present program.

The stress-measurement phase of the present program must necessarily duplicate some of this previous work, not with the intent of providing a large material survey, but in order to provide reproducible stress measurements to verify stress addition models and failure mechanisms. Following the work of Ennos, a laser interferometer technique was chosen

for the measurement of the deflection of a thin glass substrate in order to obtain the stress levels in a growing film although, as explained in Section 2.2.1., substantial modifications have been made to the Ennos type of interferometer, resulting in a more stable configuration with some unique features not previously utilized in stress-measurement applications.

2.2 STRESS-MEASUREMENT SYSTEM

The principle problem occurring in any of the stress-measurement techniques mentioned previously is a thermal one. The amount of bending detected in a beam or disc is due to both the buildup of intrinsic stress in the depositing film and, also, to any nonuniform temperature existing across the thickness of the disc. Thermal energy from the source, heaters, and shutters all provide disturbing thermal fluxes during a film deposition, and extreme care must be taken to understand and compensate for these disturbances if reproducible measurements are to be made.

The use of large discs or beams of extremely small cross section increases stress-measuring sensitivity but also increases sensitivity to temperature, vibration and particularly relief of built-in stresses in the glass discs when heated. Because we are primarily concerned with stress measurements in thick films, thicker glass substrates can be utilized, and this tends to minimize vibration and thermal influences.

At the outset of the program, a list of required measurement capabilities was established to enable stress measurements to be made for both single and multilayer films deposited under the kinds of conditions found in practice in fabricating 10.6-micron antireflection coatings. These capabilities included the use of:

- Multiple stress interferometers to enable stress measurements to be made for <u>different</u> film materials on <u>different</u> substrates during the same evaporation cycle by the use of remote shutters
- Accurate deposition rate control by the use of a crystal film-thickness monitor
- Variable vapor-incidence angles possible at each interferometer
- The inclusion of rigid substrate (KCl) at equivalent deposition positions and incidence angles
- Both electron-gun sources and resistance sources
- Accurate optical film-thickness monitoring using a white-light source and spectral filter or monochromator
- Enclosed heater assembly to maintain the interferometers, optical monitor, and rigid substrates at elevated temperatures up to 250°C

- Fabrication of semiautomatic data acquisition system to enable substrate deflection data and optical film thickness to be recorded onto paper tape for subsequent computer data reduction

Four individual interferometers were designed and fabricated and mounted onto a 36-inch stainless-steel box coater to enable the stress behavior of different combinations of two or more thin-film materials to be investigated during a single pumpdown. Using remote shutters and four interferometers, one can obtain stress data for materials A and B alone as well as for materials B on A and A on B on four different flexible and rigid substrates. The details of the interferometer design, coating chamber configuration, and data processing equipment are briefly described in the following paragraphs.

2.2.1 Cat's-Eye Stress Interferometer

The original interferometer used by Ennos to determine film stresses consisted of a Michelson interferometer detecting deflections of a thin glass beam supported at both ends by ceramic knife-edges. A set of line fringes is produced by this interferometer, and the amount of stress can be calculated from the direction and number of the fringes that move past a detector as the film is deposited. This type of interferometer was found in practice to be extremely vibration-sensitive and has been replaced by a cat's-eye interferometer developed recently at Perkin-Elmer.

The cat's-eye interferometer shown in Figure 1 produces a set of circular fringes in the return beam that are produced by interference between light reflected from the reference-reflector coating on the base of the cat's-eye lens and light reflected from a metal coating on the upper surface of a thin glass disc. When a coating is deposited onto the lower surface of the disc, the circular fringes either expand outwards or contract towards the center of the return beam, depending upon whether the stress is tensile or compressive. A change in the number of fringes and their direction of motion is detected by a silicon detector placed in a portion of the return beam. Although this interferometer detects changes in the spacing between the reflector-coated base of the cat's-eye lens and the metal-coated glass disc, its sensitivity to angular changes (vibrations) of the glass disc is greatly minimized.

The base of the cat's-eye lens is polished to a large radius surface to maintain a minimum separation of 50 to 100 microns between the reference reflector and the glass disc; this distance is also arranged to be within the depth of focus (λF^2) of the focussed beam at these two surfaces. If the two surfaces coincided exactly, the spherical reflected waves would slide inside one another as the glass disc was rotated, producing a shearing of the output beam but no change in the fringe pattern. For small separations ($\sim$100 microns) between the reference mirror and the glass disc, the effect of an angular change ($\delta\theta$) is extremely small, amounting to a change in optical path between the two primary point sources of OPD = $D\Delta\theta^2/2$, where D is the separation between the two mirror surfaces. In a similar manner, small changes in incident

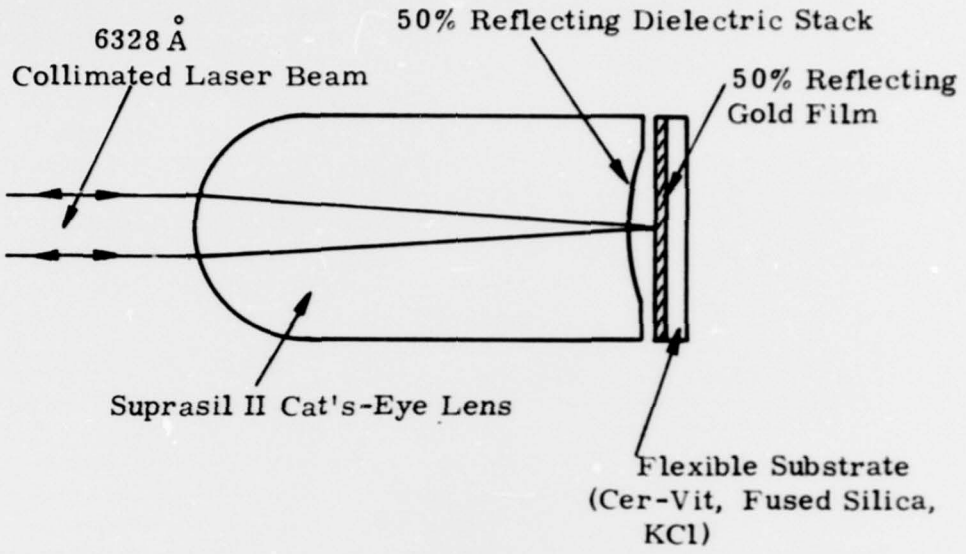

Figure 1. Cat's-Eye Interferometer

angle of the input beam cause only a minute shearing of the component wavefronts that form the output fringe pattern.

The cat's-eye interferometer lens is fabricated from fused silica or Suprasil II, and its lower surface is coated with a 50% hard dielectric coating. The convex upper surface is also coated with a broadband antireflection coating at 6328Å. Flexible substrates are fabricated from Cer-Vit, fused silica and potassium chloride in a range of thicknesses from 0.25mm to 1.0mm and are gold-coated on one side to provide a matching reflectivity of 50% to provide maximum contrast in the return fringes. Thin, semitransparent gold was chosen for coating the upper surface of the flexible substrates since it provides a low-stress film and will also withstand high-temperature vacuum baking.

The interferometer is illuminated with a 4mm diameter collimated laser beam (6328Å) produced by the interferometer laser source illustrated in Figures 2a and 2b. The polarized beam from a 2mwatt He-Ne laser is chopped by a synchronous chopper wheel and expanded to 4mm diameter by a beam expander and spatial filter. A polarizing beamsplitter reflects approximately 1% of the "p" polarized laser beam to a silicon synchronous reference detector and transmits the remaining energy to the cat's-eye interferometer. A quarter-wave plate located between the polarizing beamsplitter and interferometer rotates the polarization from "p" to "s" after two passes, and the return fringe pattern is reflected by the polarizing beamsplitter to a fringe-count detector and display screen. The polarizing beamsplitter/quarter-wave plate system is used only to maximize the amount of light on the viewing screen and is not fundamental to the operation of the interferometer system.

2.2.2 Interferometer Configuration for Variable Vapor-Incidence Angles

Since stress levels in deposited films of certain materials are known to change with vapor-incidence angle, it is desirable to configure the interferometers inside the chamber such that four different vapor-incidence angles can be accommodated with minimal interferometer realignment. The addition of two small fold mirrors to the interferometer mount, together with an offset in angle of the cat's-eye interferometer such that its axis passes through the vapor source, allows incidence angles to be easily changed. Figure 3a illustrates this configuration and Figure 3b shows a photograph of the array of interferometer heads assembled inside a heater enclosure in the 36-inch box coating unit.

The vapor-incidence angles attainable with either an electron-gun or resistance source located in the center of the chamber are variable at each interferometer between 0° and 42° with the existing tooling. The four positions allocated for rigid substrates are positioned on the same radius as the interferometer heads, and the vapor-incidence angles of the rigid substrate can also be set to any angle between 0° and 45°.

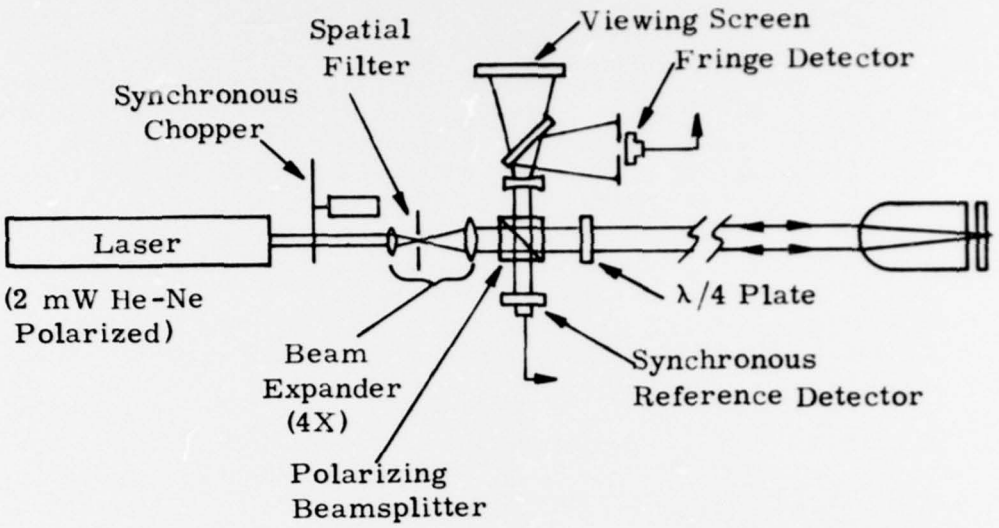

Figure 2a. Stress Interferometer Configuration

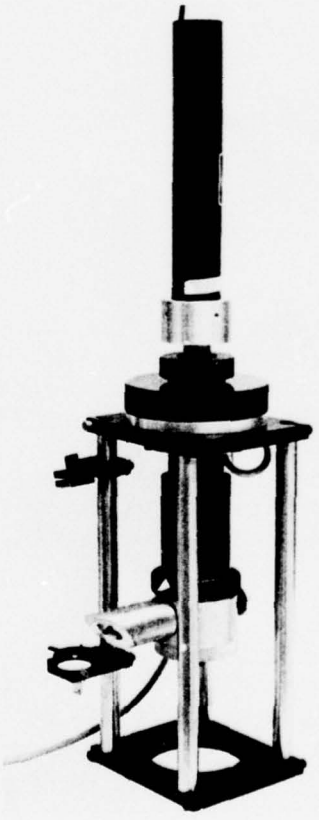

Figure 2b. Laser Interferometer Source

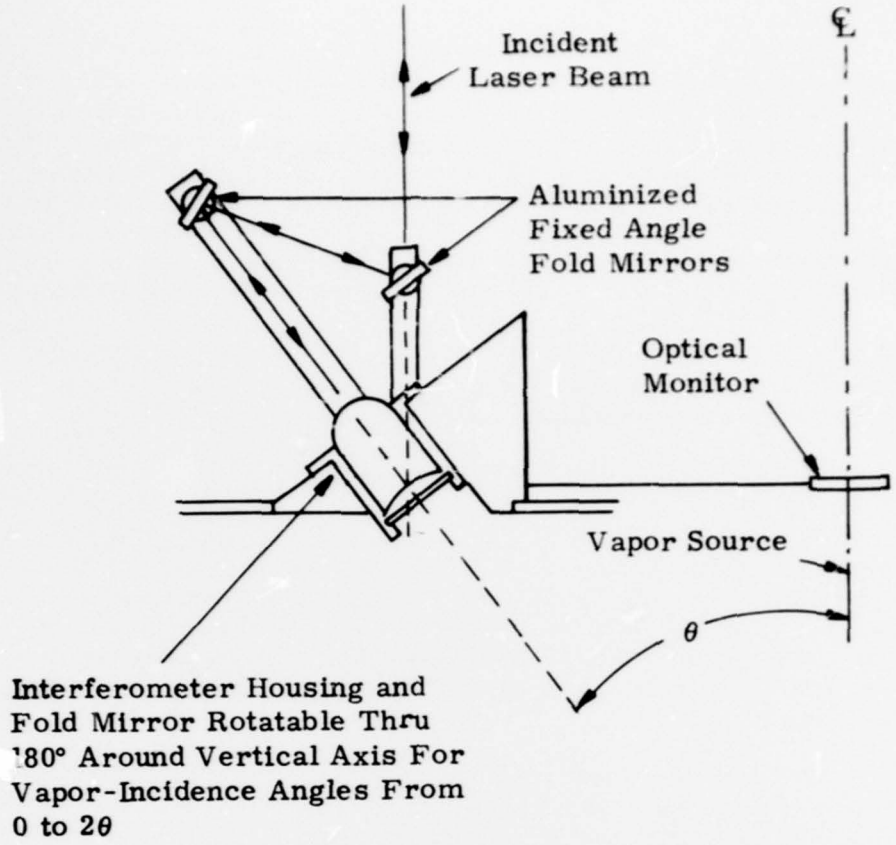

Figure 3a. Variable Vapor-Incidence Angle Configuration

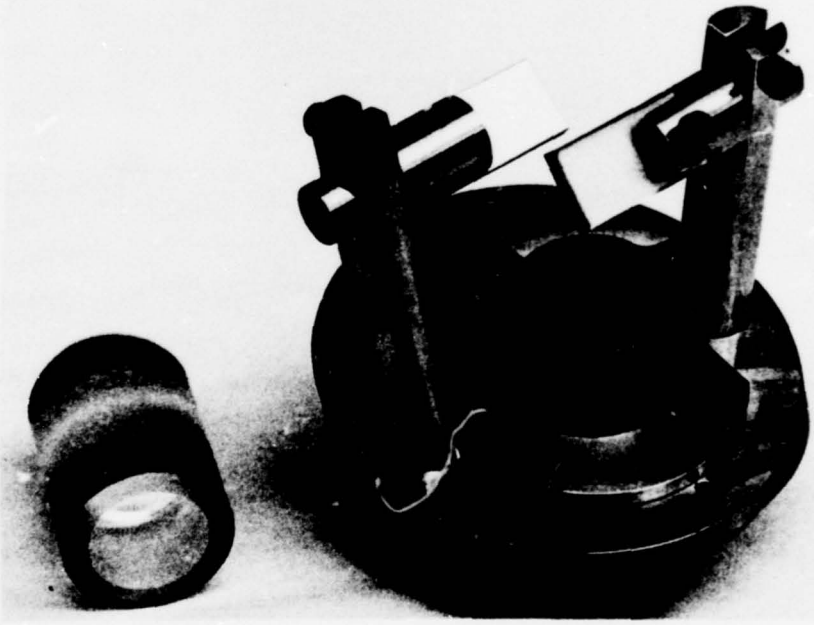

Figure 3b. Stress Interferometer Array with Variable Vapor-Incidence Angle Fold Mirrors

An optical-thickness monitor is located on the centerline of the chamber, and optical film thicknesses are monitored at any desired wavelength up to 1.0 micron by suitable choice of line filters. Optical thicknesses of the composite films of multilayers are individually monitored using fresh glass microscope slides for component films during an evaporation cycle.

The entire assembly of interferometers, rigid substrate holders, and optical monitor slides are enclosed in stainless-steel shields and can be heated to 250°C by a Calrod heater located at the top of the vacuum chamber, Figures 4a and 4b. Temperature control is obtained using an SCR proportional controller and thermistor mounted close to the interferometer housings.

2.2.3 Data Acquisition and Data Recording System

Stress changes in the depositing films cause the bull's-eye fringe patterns at the fringe-count detector to expand or contract depending upon the nature of the stress (tensile or compressive). Changes in intensity of the central fringe are detected by PIN diodes and are fed to lock-in amplifiers that synchronously demodulate the chopped signals using a reference signal from a second silicon diode in the laser source housing.

The output of the optical monitor and stress interferometers are recorded on a six-channel chart recorder and are also applied to the input of a datalogger/paper-tape recorder. Figures 5a and 5b illustrate the function and form of the data recording system.

The recording system datalogger can be arranged to scan the five input channels at two fixed speeds of two channels/second or seven channels/second, the first channel always being the elapsed time. These two speeds in combination with the use of different glass thicknesses for the flexible substrate allow sufficient sampled data points to be recorded per fringe over a wide range of stress levels.

2.3 STRESS-MEASUREMENT SYSTEM - OPERATIONAL CHARACTERISTICS

Initial tests of a single stress interferometer mounted to the vacuum system showed that:

- Stable bull's-eye fringes were formed at the display screen and fringe-count detector and pump vibration was not a disturbing factor.
- High quality two-beam interference fringes are projected onto the detector and changes in the fringes are recorded with great fidelity.
- Although heating the vacuum system to 250°C causes the fringe count to change due to nonuniform heating of the glass disc, the fringe system is reproducible, stable, and of high contrast when the system reaches thermal equilibrium.

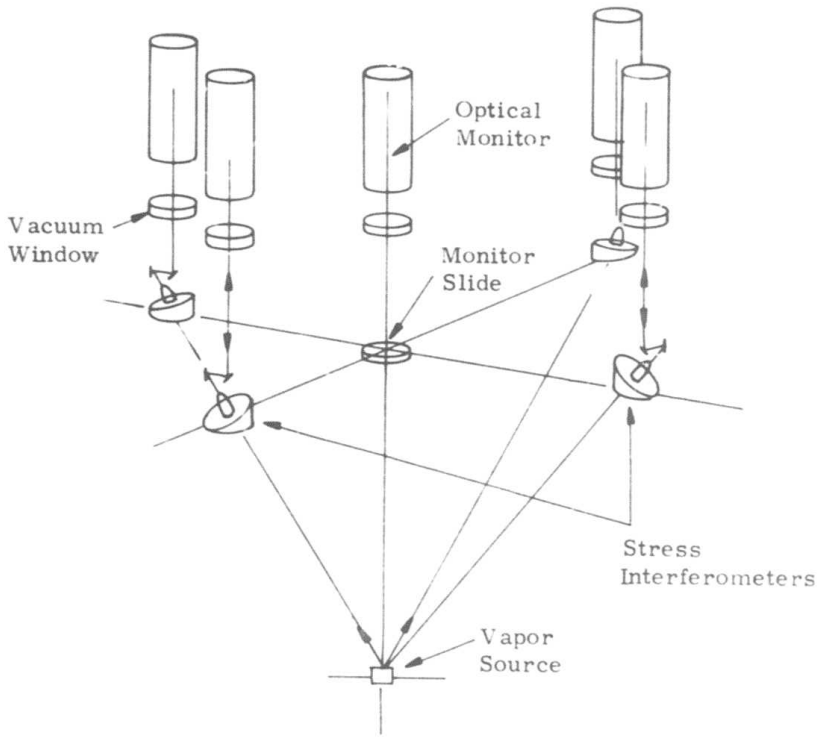

Figure 4a. Interferometer and Optical Monitor Configuration in a Vacuum System

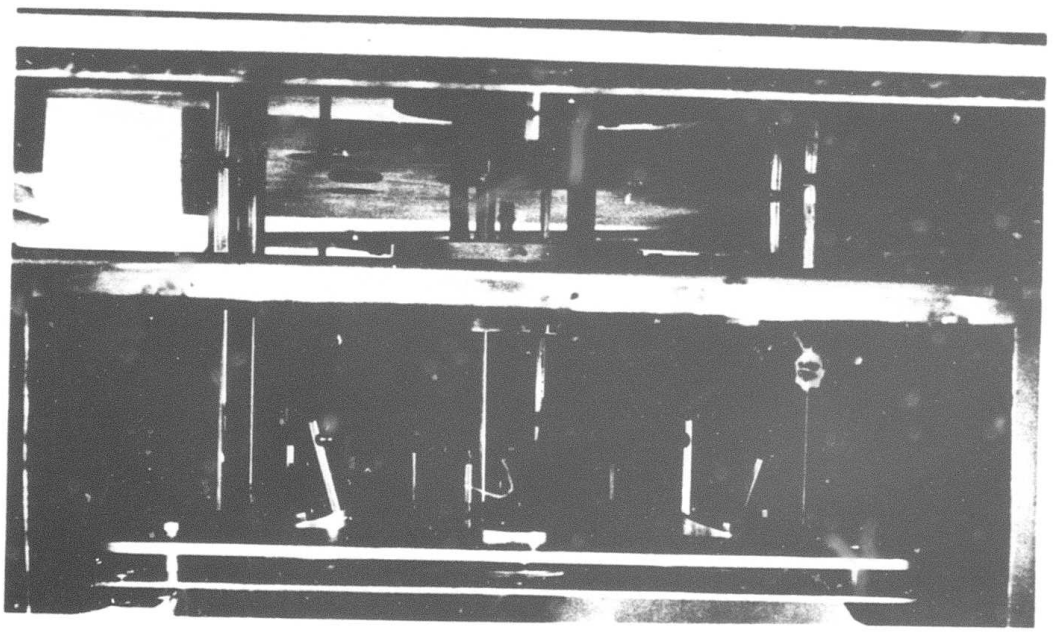

Figure 4b. Stress-Interferometer Assembly Inside Heated Enclosure

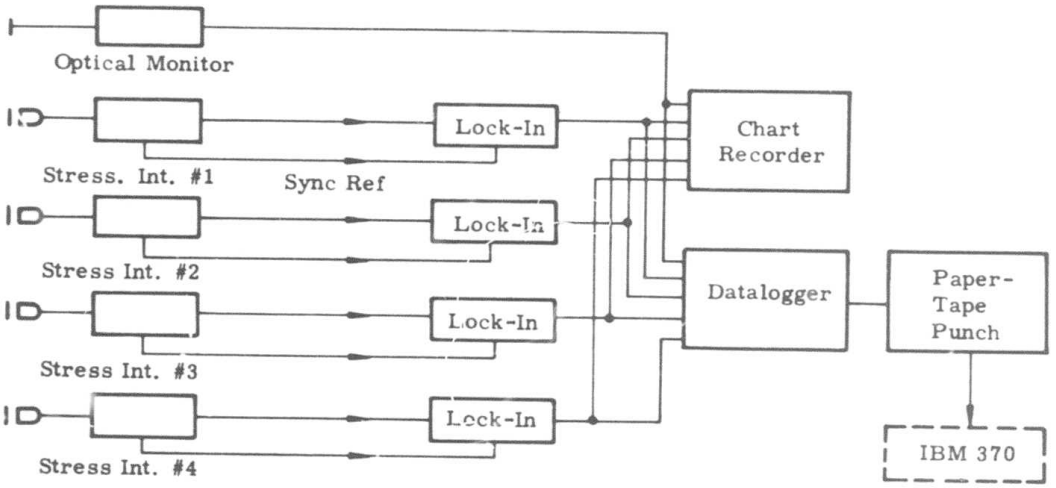

Figure 5a. Interferometer Data Acquisition and Recording System

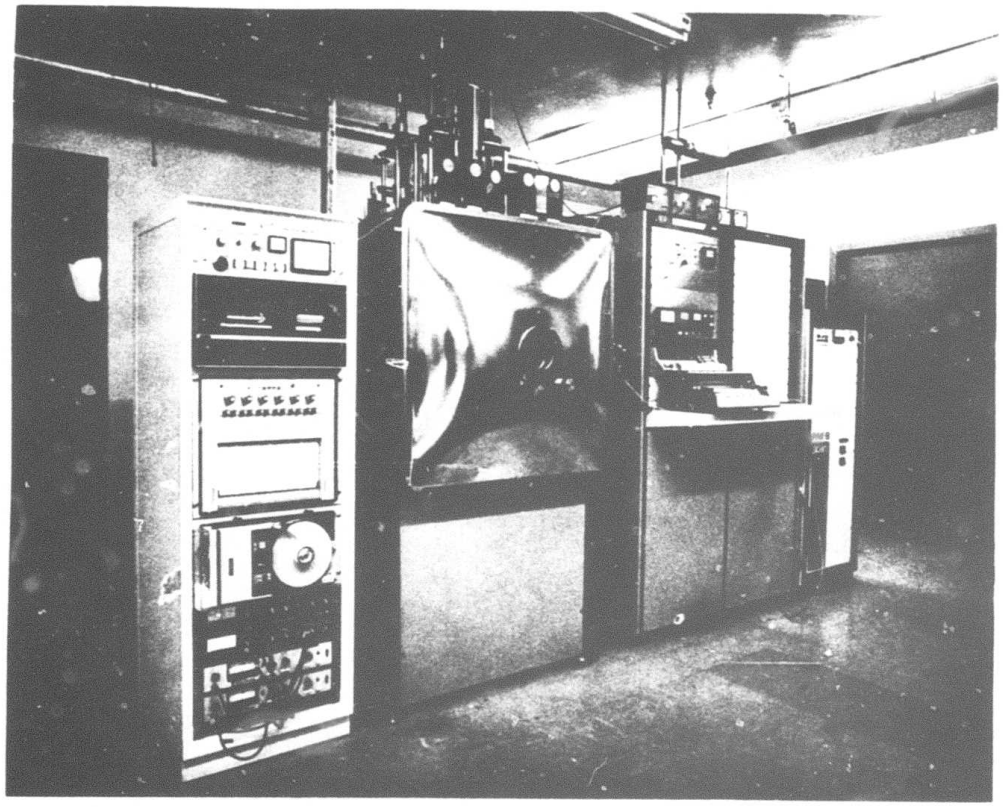

Figure 5b. Stress-Measuring Interferometer System with Data Recording Instrumentation

Figure 6 shows a typical fringe pattern (overexposed) produced at the detector (PIN-10 diode) and display screen; the detector's sensitive area is aligned with the center of the fringe pattern and detects intensity changes as fringes grow from or disappear into the center of the fringe pattern. Figure 7a shows the change in intensity or fringe count for a thin glass disc 0.25 mm thick at 200°C being coated with thorium fluoride evaporated from an electron-gun source. The fringe change contains an amplitude modulation due to material being deposited onto the second surface of the flexible disc. The use of a gold semitransparent film to provide a reflectivity of 50% at 6328Å on the upper surface of the flexible disc, together with the 50% reference reflector, forms a three-mirror cavity and leads to amplitude modulation with deposited film thickness in the reflected beam. Although this could be used to measure the deposited film thickness, it is not used in practice since the fringe counts obtained for thicker glass slides are generally of longer period than the optical thickness changes.

A more interesting and potentially more useful feature of fringe-pattern recording is a waveform asymmetry that occurs each cycle and depends upon the direction of fringe motion. The slopes of the waveform at the two zero crossing points per cycle are not equal, and a correspondence between the slopes and the direction of fringe motion, and consequently, plate deflection direction can be established. Figure 7b illustrates this behavior for a film of magnesium fluoride deposited onto Cer-Vit at room temperature. As the film thickness increases from zero, the positive-going slope is greater than the negative-going slope, corresponding both to fringes moving outwards from the center of the fringe pattern and to a tensile stress. At the point indicated, the film breaks and the deflection reverses in sign; the fringes collapse into the center of the pattern; and stress-relief occurs corresponding to a stress reduction in the film. After film rupture, the positive-going slope is less than the negative-going slope, and this slope change with fringe direction can be utilized during data reduction to obtain the nature sign of the stress in the depositing film.

The asymmetry of the output waveform is not due to angular alignment errors in the fringe pattern and detector system but is quite reproducible and is a basic property of the interferometer configuration. This effect cannot be completely explained at this time, but it does disappear when the detector aperture only samples a small area at the center of the fringe pattern corresponding to the interferometer operating in collimated light. The interferometer forms circular fringes by the coherent addition of multiple focussed Gaussian beams, and this focussed configuration is thought to produce the wavefrom asymmetry, although, at present, this has not been theoretically investigated.

The initial test of the interferometer showed that a stable and reproducible fringe count is obtained, and a system of four interferometers was constructed and mounted on the vacuum system. Figure 8 shows the chart recording for a typical stress-measurement experiment

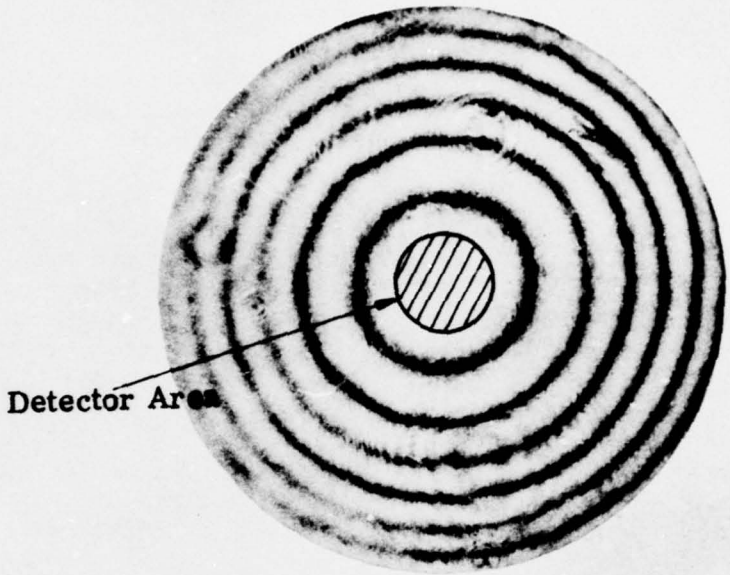

Figure 6. Fringe Pattern at Output of Stress-Measuring Interferometer

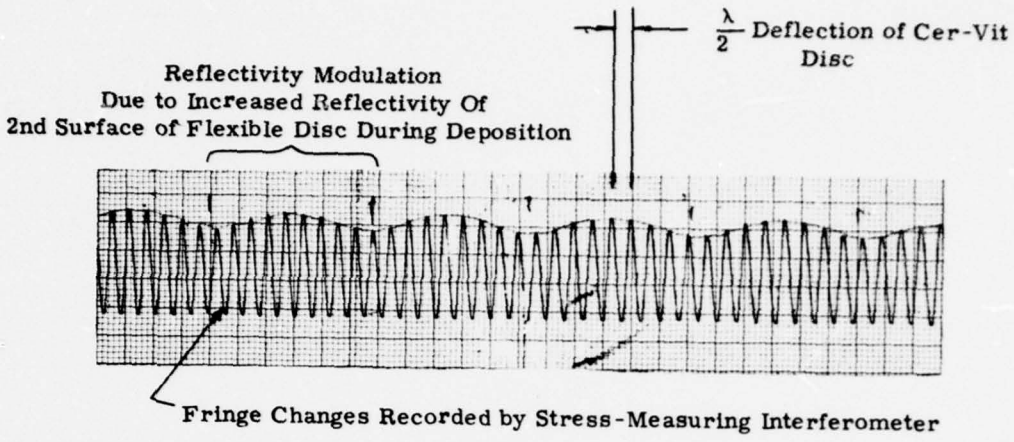

Figure 7a. Intensity Variations (Fringe Count Due to ThF_4 Film Being Deposited onto a 0.25-mm Cer-Vit Disc)

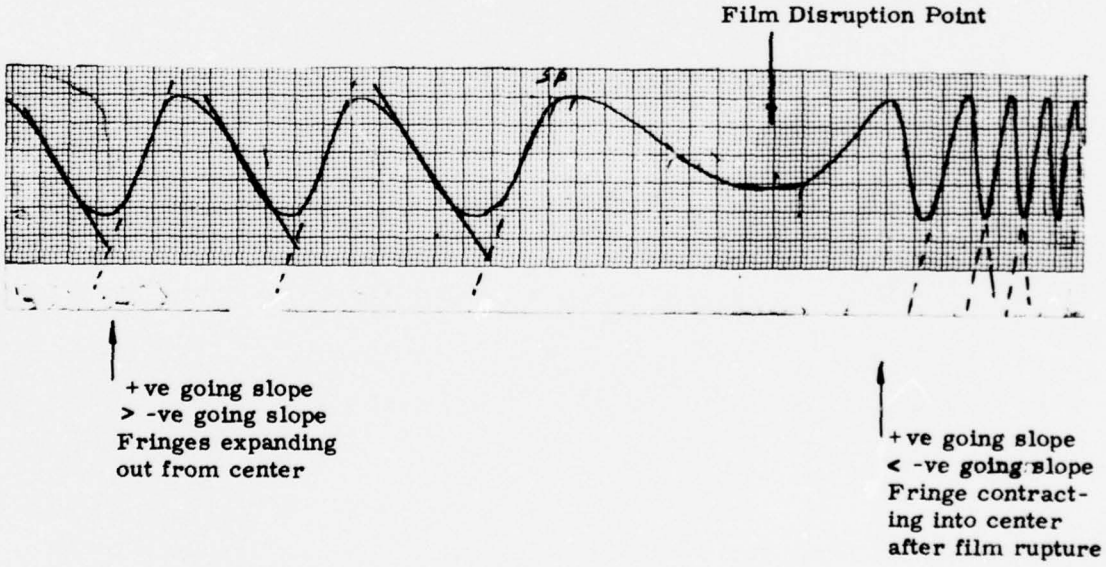

Figure 7b. Fringe Count for a 0.5-mm Thick Cer-Vit Disc During Deposition of MgF_2 (Note waveform asymmetry indicating direction of fringe motion before and after film cracking)

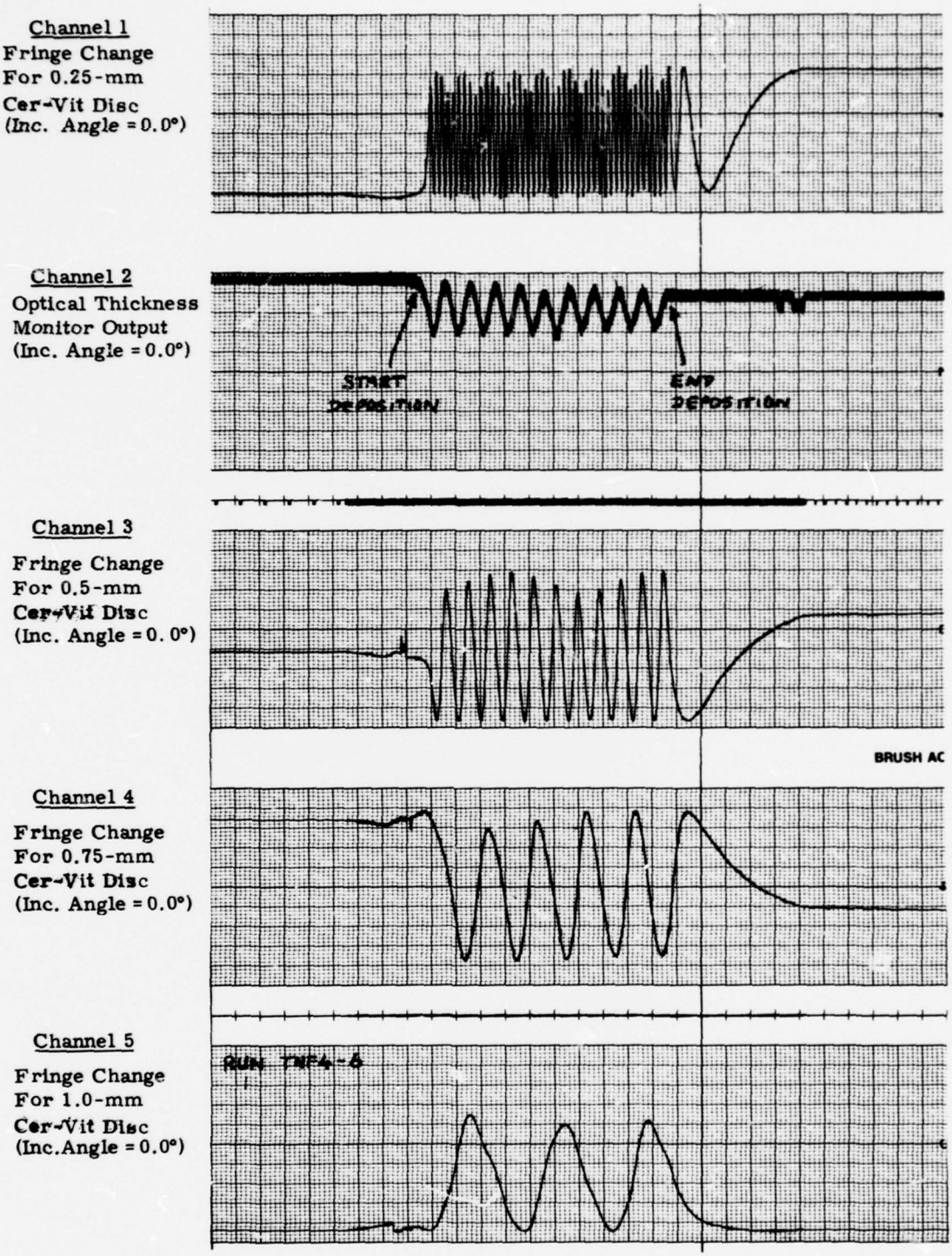

Figure 8. Data Recording for Four Simultaneous Stress Measurements for ThF_4 Deposited onto Cer-Vit Discs of Varying Thicknesses at 200°C

using thorium fluoride deposited onto Cer-Vit discs of various thicknesses at 200°C. The second channel is the optical thickness of a monitor slide located in the center of the chamber. The fringe changes are simultaneously recorded onto paper tape, and the sampled data is processed using an IBM 370 after deposition is completed.

2.4 FILM STRESS DATA REDUCTION

The total number of sampled data points per channel is nominally 250 (data rate of 2 channels/second) for the entire deposition run, but this can be varied by changing the recording speed and/or the glass disc thickness. This number of data points is typical for the deposition of $\lambda/4$ films at 10.6 microns, although a data rate of 7 channels per second is available from the datalogger/tape-punch unit.

The recorded data is processed to yield the stress in the film deposited onto each disc, and the data reduction calculates the average stress $\langle S_i \rangle$ for the i^{th} disc according to

$$\langle S_i \rangle = \frac{4E_i\omega_i}{3(1-\nu_i)} \left(\frac{h_i}{D_i}\right)^2 \frac{1}{t_m \delta_i}$$

where

E_i = Young's modulus of i^{th} disc

ν_i = Poisson's ratio of i^{th} disc

h_i = Thickness of i^{th} disc (mm)

D_i = Diameter of i^{th} disc (mm)

ω_i = Deflection due to stress $\langle S_i \rangle$ of i^{th} disc (microns)

t_m = Mechanical thickness of film deposited on monitor slide

δ_i = Distribution factor for i^{th} slide (ratio of thickness on i^{th} slide to thickness of film on optical monitor)

The deflections (ω_i) are obtained from the sample data by the following computational steps:

(1) Normalize all channels to the maximum reading occurring during deposition.

(2) Locate zero crossing points.

(3) Normalize individual cycles to unity.

(4) Calculate mechanical deflections.

(5) Differentiate deflections and sum absolute values.

The mechanical thickness of the film deposited onto the optical monitor is also calculated in a similar manner and, together with the distribution factors (δ_i) and the optical deflections (ω_i), is used to calculate the average stress $\langle S_i \rangle$ for each point recorded. The data computed in this manner is interpolated to provide stress level as a function of the mechanical film thickness deposited onto each substrate. Figure 9 shows the data reduction for the curves shown in Figure 8 for a thorium fluoride film deposited onto Cer-Vit discs of various thicknesses. Evaporation rates are automatically calculated for each channel together with the number of fringes calculated by the data-reduction program and serve as a check on the experimental conditions. The optical monitor input from the Balzer monitor is an extremely noisy signal resulting in double maxima and minima, and the fringe count for Channel 2 is computed incorrectly as are the variations of thickness with time. Since the noise is uniform throughout the recording and since the optical film thickness is deposited as an exact number of quarter-waves at some preselected monitor wavelength, the thickness data is linearly scaled to the correct thickness.

The entire interferometer system was used for a series of preliminary experiments designed to check out the entire system under operational conditions, and thorium fluoride (ThF_4) was selected as the thin-film material because of its wide use in laser coatings in the 10-micron region.

2.5 STRESS EVALUATION OF THORIUM FLUORIDE FILMS - EXPERIMENTAL RESULTS

The calculation of stress utilizing the equation given in Section 2.4 assumes that:

(1) The deposited film thicknesses are small compared to the flexible substrate thickness.

(2) The measurement is independent of the substrate material chosen.

(3) The measurement is independent of the substrate thickness.

(4) No stress relief occurs in the substrate/film combination and no slippage occurs at the film/substrate boundary.

The first condition is satisfied for $\lambda/4$ films in the 10-micron region (t = 1 to 2 microns) as described here since the flexible glass substrates used range from 250 to 1000 microns in thickness. The dependence, if any, of the stress measurement upon the thickness and type of substrate material used can be checked using the present four-channel interferometer system. The final condition is more difficult to verify experimentally, but calculations given in Section 3 show that the effects of stress relief are small for thick films. Since the interferometer system can measure the stress on four different thickness materials or on different substrates in the same vacuum deposition, the second and third conditions can be checked experimentally.

STRESS DATA ANALYSIS

RUN NO 11 DEC 22 THF4 200C 0.25,0.5,0.75,1.0 PM CRYVIT /CH/SEC

F' NAME = THF4-6

INPUT DATA LIMITS

	CHANNEL 1	CHANNEL 2	CHANNEL 3	CHANNEL 4	CHANNEL 5
MAX REC VOLTAGE	7.504	0.093	7.786	0.893	0.952
MIN REC VOLTAGE	0.770	0.066	0.295	0.131	0.054

SUBSTRATE PARAMETERS

	CHANNEL 1	CHANNEL 2	CHANNEL 3	CHANNEL 4	CHANNEL 5
SUB MATERIAL	1		1	1	1
WEIGHT (GMS)	0.324		0.616	0.983	1.295
SUB THICKNESS (MM)	0.256		0.486	0.778	1.022
DIST(CON) FACTOR	0.733		0.693	0.712	0.761

***** FILM DEPOSITED = 20 QUARTER WAVES OF INDEX 1.48 AT 0.804 MICRONS *****

SUBSTRATE DEFLECTION (MICRONS)
(CHANNEL 2 IS OPTICAL MONITOR)

CHANNEL 1	CHANNEL 2	CHANNEL 3	CHANNEL 4	CHANNEL 5
0.089	0.018	0.000	0.001	0.0
0.128	0.085	0.014	0.053	0.026
0.530	0.238	0.098	0.077	0.053
0.949	0.334	0.234	0.100	0.077
1.424	0.425	0.338	0.131	0.102
1.848	0.562	0.432	0.174	0.142
2.277	0.630	0.571	0.221	0.200
2.750	0.732	0.669	0.269	0.230
3.164	0.849	0.771	0.329	0.251
3.639	0.963	0.908	0.387	0.267
4.075	1.065	1.004	0.424	0.288
4.527	1.159	1.119	0.464	0.314
4.985	1.294	1.245	0.508	0.333
5.407	1.439	1.335	0.566	0.369
5.896	1.529	1.471	0.628	0.408
6.328	1.619	1.579	0.692	0.439
6.777	1.789	1.677	0.734	0.472
7.211	1.869	1.810	0.769	0.499
7.641	1.969	1.911	0.809	0.528
8.113	2.113	2.008	0.864	0.575
8.543	2.207	2.152	0.927	0.606
9.017	2.316	2.250	0.997	0.631
9.450	2.389	2.351	1.042	0.649
9.903	2.500	2.496	1.083	0.670
10.366	2.644	2.589	1.124	0.702
10.794	2.726	2.700	1.169	0.729
11.274	2.845	2.836	1.229	0.753
11.707	3.047	2.934	1.296	0.784
12.181	3.162	3.065	1.348	0.826
12.616	3.305	3.176	1.393	0.844
13.062	3.418	3.280	1.434	0.866
13.527	3.489	3.421	1.455	0.881
TOTAL NO OF MAX AND MINIMA	89	43	22	11	6
DEPOSITION RATE (A/SEC)	33.298	45.120	31.259	32.125	34.341

STRESS DATA REDUCTION

STRESS LEVEL KG/CM.CM CHANNEL 1	FILM THICKNESS (MICRONS) CHANNEL 2	STRESS LEVEL KG/CM.CM CHANNEL 3	STRESS LEVEL KG/CM.CM CHANNEL 4	STRESS LEVEL KG/CM.CM CHANNEL 5
493.298	0.100	325.567	1056.967	988.950
844.449	0.200	840.033	1082.098	1110.024
997.819	0.300	869.900	864.405	1130.459
1063.054	0.400	1019.449	1017.345	1413.394
1062.796	0.500	1030.502	1041.425	1300.378
1119.274	0.600	1076.329	1126.196	1209.027
1111.544	0.700	1083.363	1087.827	1197.379
1101.019	0.800	1082.046	1104.713	1197.329
1125.314	0.900	1081.014	1164.520	1236.663
1099.402	1.000	1079.173	1137.699	1187.240
1114.111	1.100	1074.896	1127.648	1202.989
1118.224	1.200	1099.796	1150.741	1243.796
1126.413	1.300	1100.098	1200.709	1237.463
1145.705	1.400	1111.325	1202.259	1219.630
1140.140	1.500	1105.[illegible]	1190.970	1210.642
1141.023	1.600	1094.943	1200.669	1206.521
1133.663	1.700	1078.218	1179.950	1185.539
1121.910	1.800	1078.699	1172.903	1156.232
1115.094	1.900	1104.969	1163.361	1171.294
1129.842	2.000	1098.263	1152.521	1134.645

Figure 9. Stress Data Reduction of Data in Figure 8, ThF$_4$-6 Deposited Onto Substrates of Various Thicknesses at 200°C

The data shown in Figures 8 and 9 gives the stress levels for ThF_4 films deposited onto Cer-Vit discs of different thicknesses of known weight and density and shows that indeed the equilibrium stress is independent of the glass substrate thickness. A similar experiment was carried out utilizing thin flexible discs of fused silica, Cer-Vit and potassium chloride to determine the effect of different substrate materials. The disc thicknesses were obtained by weighing, and the elastic constants for each material used in the data reduction are shown in the table below.

Material	Young's Modulus (E)	Density (ρ)	Poisson's Ratio (ν)
Cer-Vit*	9.23×10^5 kg/cm^2	2.5 gm/cm^3	0.25
Fused Silica**	7.00×10^5 kg/cm^2	2.2 gm/cm^3	0.17
KCl†	3.02×10^5 kg/cm^2	1.98 gm/cm^3	0.11

* Owens-Illinois Data
** Corning Glass Works Data
† L.S. Combes, S.S. Ballard, and K.A. McCarthy, JOSA, 41, 215 (1951).

The stress data measured for ThF_4 using two KCl substrates (1.0mm thick), a 0.5mm thick fused silica substrate and a 0.5mm thick Cer-Vit substrate are shown in Figure 10. The stress levels calculated for fused silica and KCl agree closely but give smaller equilibrium stress levels than that measured using Cer-Vit. This difference (~ 10%) in stress measurements is reproducible and is probably caused by a value of Young's modulus for Cer-Vit that is too high. The small discrepancy is not considered significant at this stage of the program, and one can conclude that intrinsic stress measurements obtained by using different substrate materials give comparable values.

2.6 STRESS CHARACTERIZATION OF THORIUM FLUORIDE SINGLE FILMS

One would expect the stress buildup in a growing thin film to be dependent upon substrate temperature, evaporation rate, and vapor-incidence angle, although many other variables (vacuum pressure, glow discharge cleaning, etc.) could contribute to the stress levels attained in practice. Clearly, the number of experimental measurements required to fully characterize the stress properties of a single material is prohibitive if all these parameters are included.

Since measurements can now be made for many combinations of substrate, film material, and incidence angle during the same coating run, the number of coating experiments required for each material can be somewhat minimized. A series of stress measurements consisting of depositions at various rates and temperatures at different vapor-incidence angles (0°, 20°, 30°, 40°) has been completed for thorium fluoride. The effects of different angles of incidence is minimal

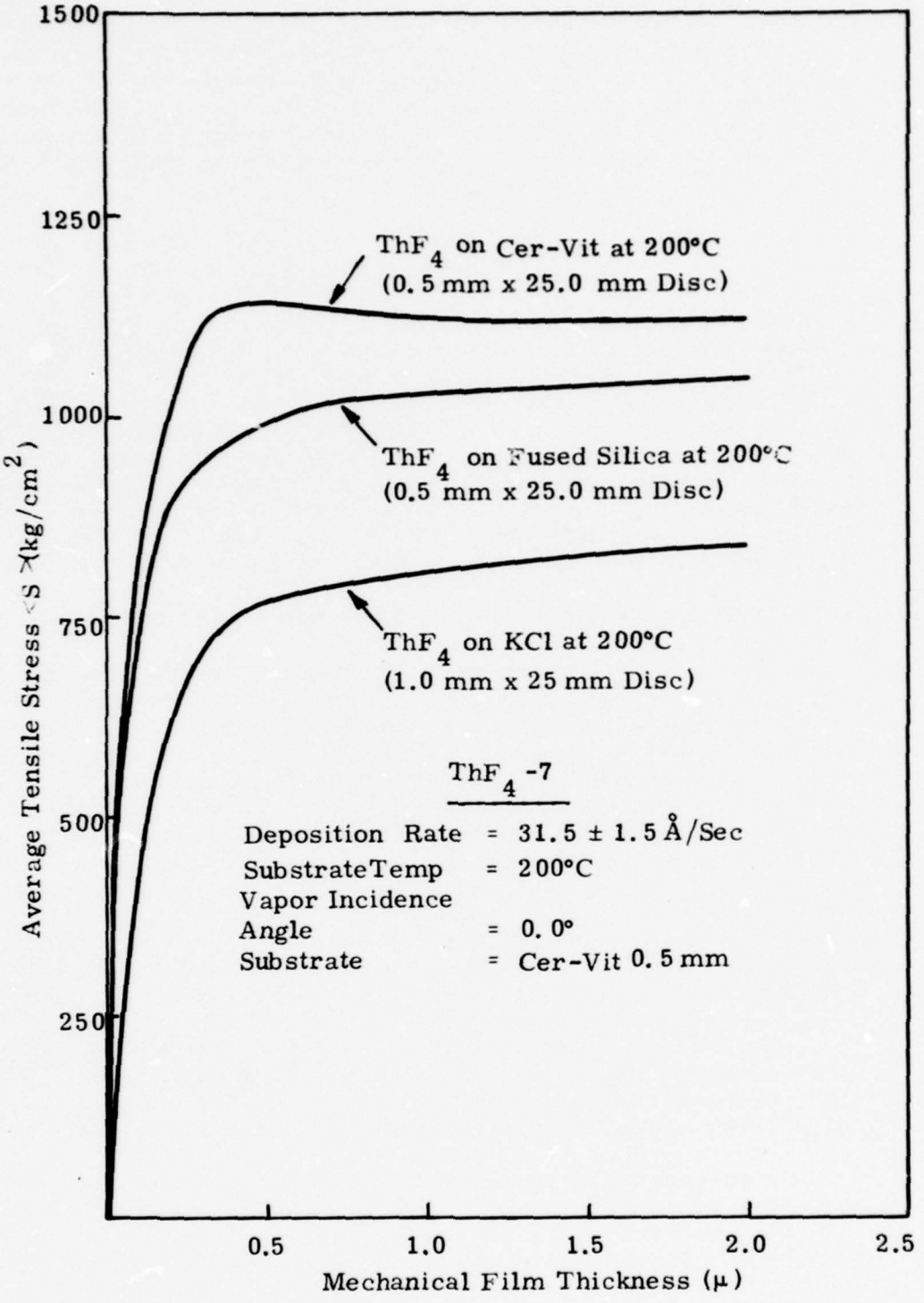

Figure 10. Instantaneous Stress Levels Computed for ThF_4 Deposited Onto Cer-Vit, Fused Silica and KCl Under Identical Conditions

for thorium fluoride as shown in Figure 11 (note that deposition rates are also dependent upon the incident angles since total film thickness is reduced at high incidence angles). The effect of different evaporation rates at a constant temperature (200°C) for thorium fluoride is shown in Figure 12. This data is for a vapor-incidence angle of 0°, but little difference is obtained for incidence angles of 20°, 30°, and 40°.

The behavior of film stress with substrate temperature is shown in Figure 13 where, once again, an equilibrium stress level is attained for all temperatures in the 100 to 200°C range. Deposition of thorium fluoride at lower temperatures was not carried out because such films possess large absorptions in the 10.0 micron region.

The variation of absorption of the component films of antireflection coating material at 10.6 microns is required during the present program, but this measurement phase will be carried out when stress measurements of entire antireflection coatings are performed later in the program. The intent during the first 6 months of the program was the design and fabrication of a semiautomated stress measurement system that will be utilized during the experimental investigation of multilayer coatings.

2.7 INVESTIGATION OF THERMALLY INDUCED STRESSES IN ThF_4 FILMS

After a single film is deposited onto a substrate at a high temperature, the substrate/film combination must be cooled to room temperature before the system is vented to the air. This cooldown cycle can induce great stress changes in the film if the thermal expansion coefficient mismatch between film and substrate is sufficiently large. The study of such thermally induced stresses becomes extremely important for coatings applied to high expansion laser window materials such as KCl since thermal stresses during fabrication and during laser heating can lead to film failure. Large thermally induced stresses present a severe problem during the fabrication of antireflection coatings as reported by Kurdock and Strouse,[11] where the deposition of antireflection coatings of $ZnSe/ThF_4$ materials onto KCl at temperatures higher than 150°C was followed by catastrophic film failure during cooldown.

Film failure, as predicted, was caused by compressive stress and delamination of the coating at the $ZnSe-ThF_4$ boundary. Similar contradictory behavior was exhibited by cerium fluoride deposited onto KCl at 250°C where, once again, compressive stresses caused film failure.

Severe heating of the coated window can also occur when exposed to high-power laser radiation, and thermally induced stresses can produce film failure before the intrinsic laser damage threshold of the material is reached. Laser heating is also spatially nonuniform, which compounds the problem of predicting film failure of a coating due to thermally induced stresses.

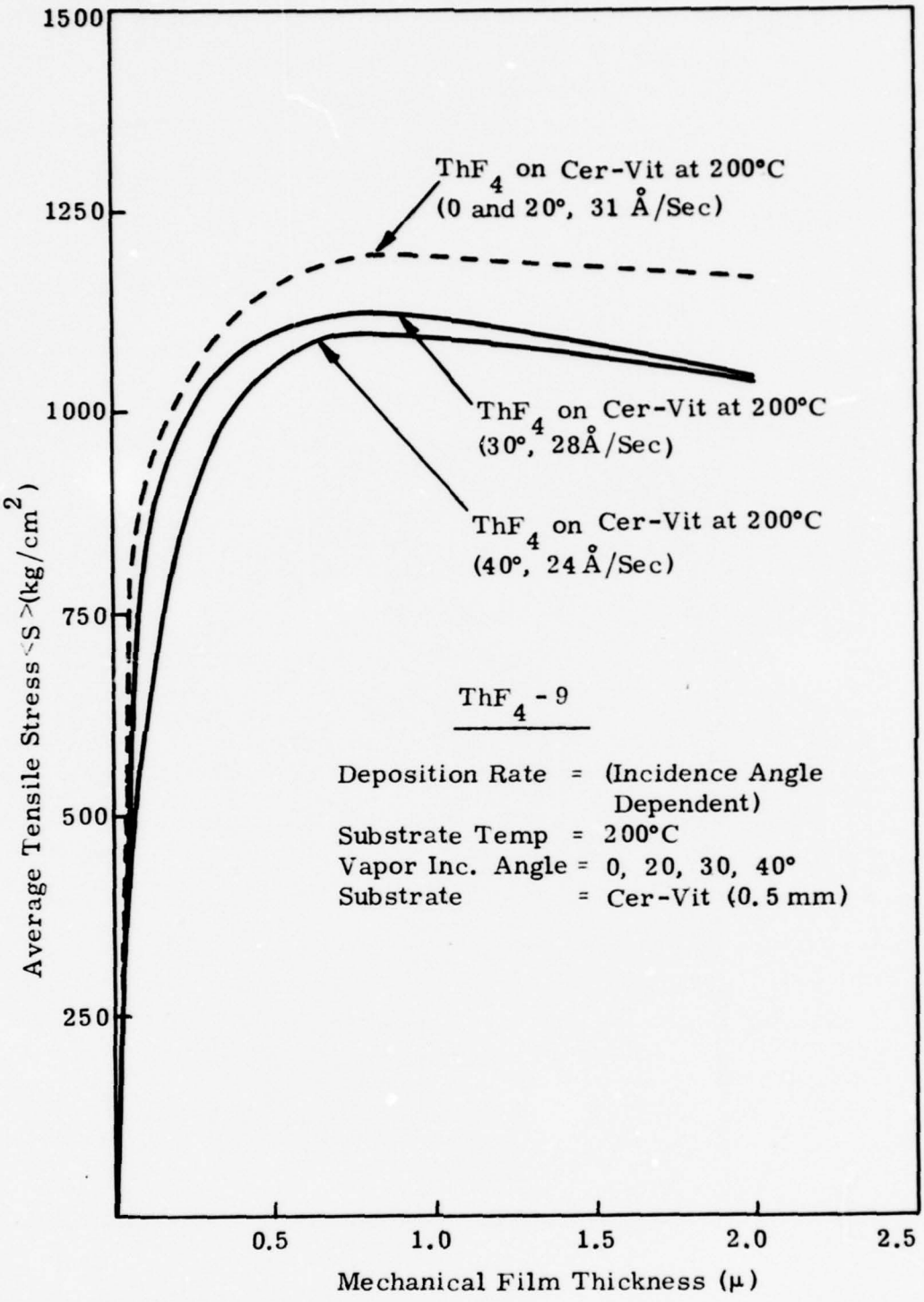

Figure 11. Dependence of Stress Buildup in ThF_4 at 200°C With Vapor Incidence Angle

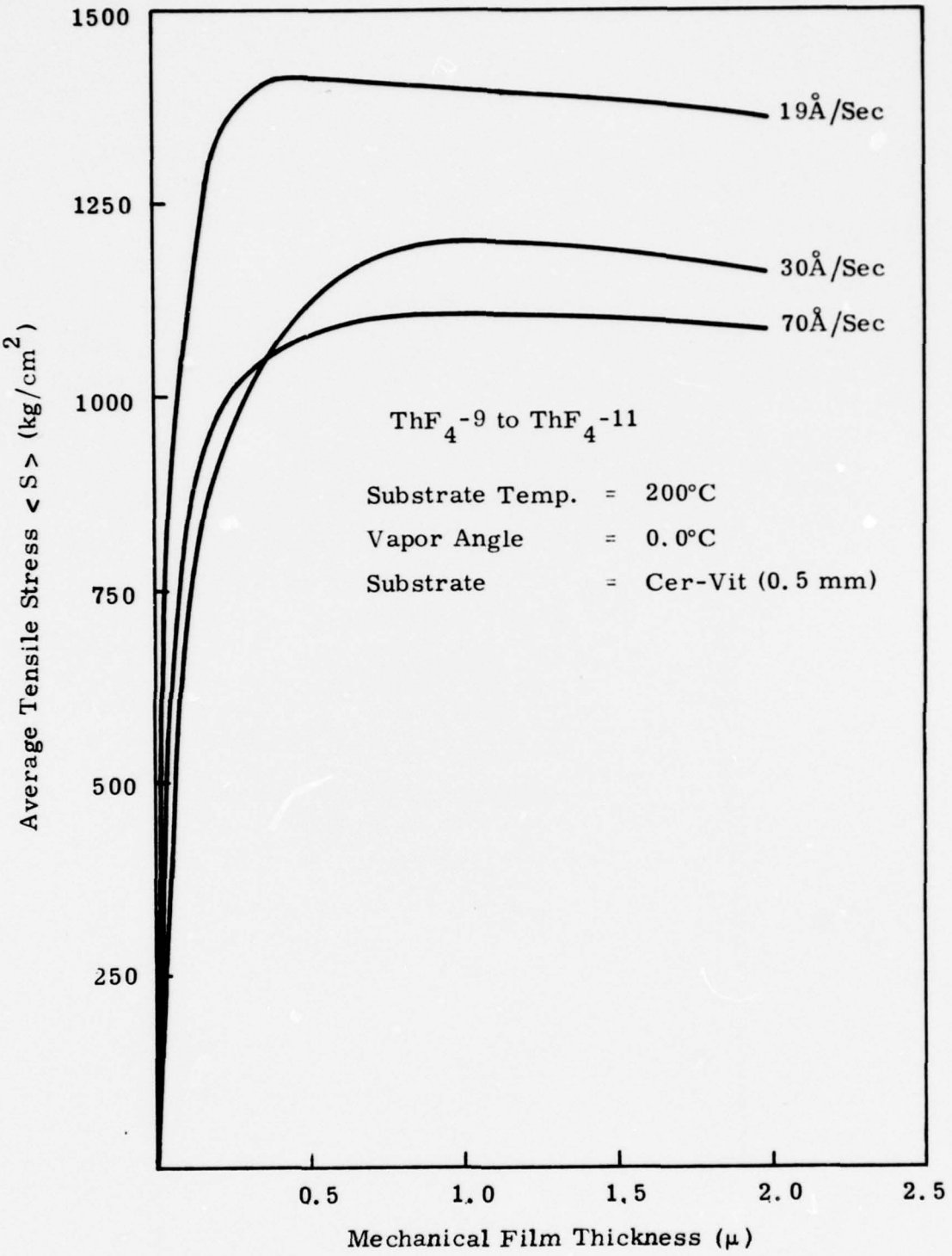

Figure 12. Stress Dependence of Thorium Fluoride Deposited at Different Evaporation Rates

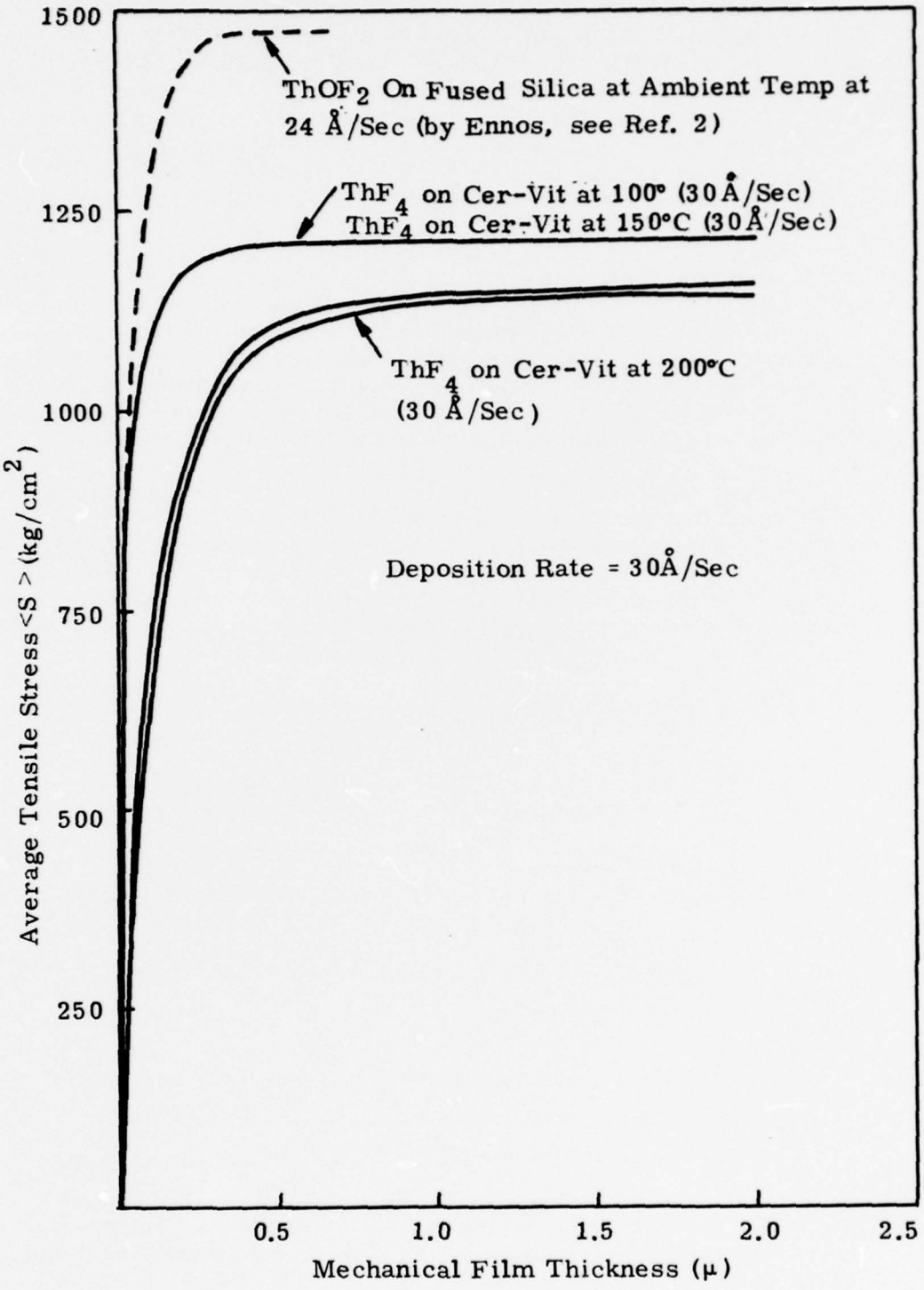

Figure 13. Stress Dependence of Thorium Fluoride Material Deposited Onto Substrates of Different Temperatures

Thermally induced stress contributions can be measured directly for an identical film deposited onto up to four different substrate materials using the stress-interferometer system. During the cooldown cycle, the fringe pattern tends to go out of alignment at the fringe-count detectors due to the contraction of the box coater shell. However, with occassional realignment by the operator, a complete fringe change history can be recorded for all channels, and the amount of deflection due to thermally induced stresses can be determined.

The results of an initial experiment using thorium fluoride films deposited onto Cer-Vit and KCl flexible substrates show that the construction of the substrate has a great effect on final film stresses after cooldown. An additional benefit of monitoring the thermal deflection of different substrate simultaneously is that Young's modulus and the thermal expansion coefficient of the thin-film material can be easily determined. These values are essential to any model of stress addition that includes temperature effects.

Figure 14 shows the change in fringe count that occurs when substrates of Cer-Vit (0.5mm thick) and KCl (1.0mm thick) coated with ThF_4 are cooled from 200°C to ambient temperature (22°C). The direction of fringe motion shows that the tensile stress in the film is greatly reduced for the KCl substrate and is greatly increased for the Cer-Vit substrate. As described below, these fringe changes can be used to determine the following important parameters:

- The resultant stress level in the thin-film coating after cooldown
- The effective values of Young's modulus and thermal expansion coefficient for the thin-film material.

The stress change produced by a temperature change ΔT in a substrate/thin-film system having different expansion coefficients is given by

$$\sigma = E_f (\alpha_f - \alpha_s) \Delta T \quad kg/cm^2$$

where

E_f = Young's modulus for the film material (kg/cm^2)
α_f = Thermal coefficient of expansion of the film
α_s = Thermal coefficient of expansion of the substrate

The deflection produced by the stress (σ) in a disc of material characterized by a thickness h, diameter D, modulus E_s and Poisson's ratio ν_s is

$$\omega = \frac{3(1 - \nu_s)\, t}{4\, E_s} \left(\frac{D}{h}\right)^2 \sigma$$

where the film thickness (t) is much less than the disc thickness (h).

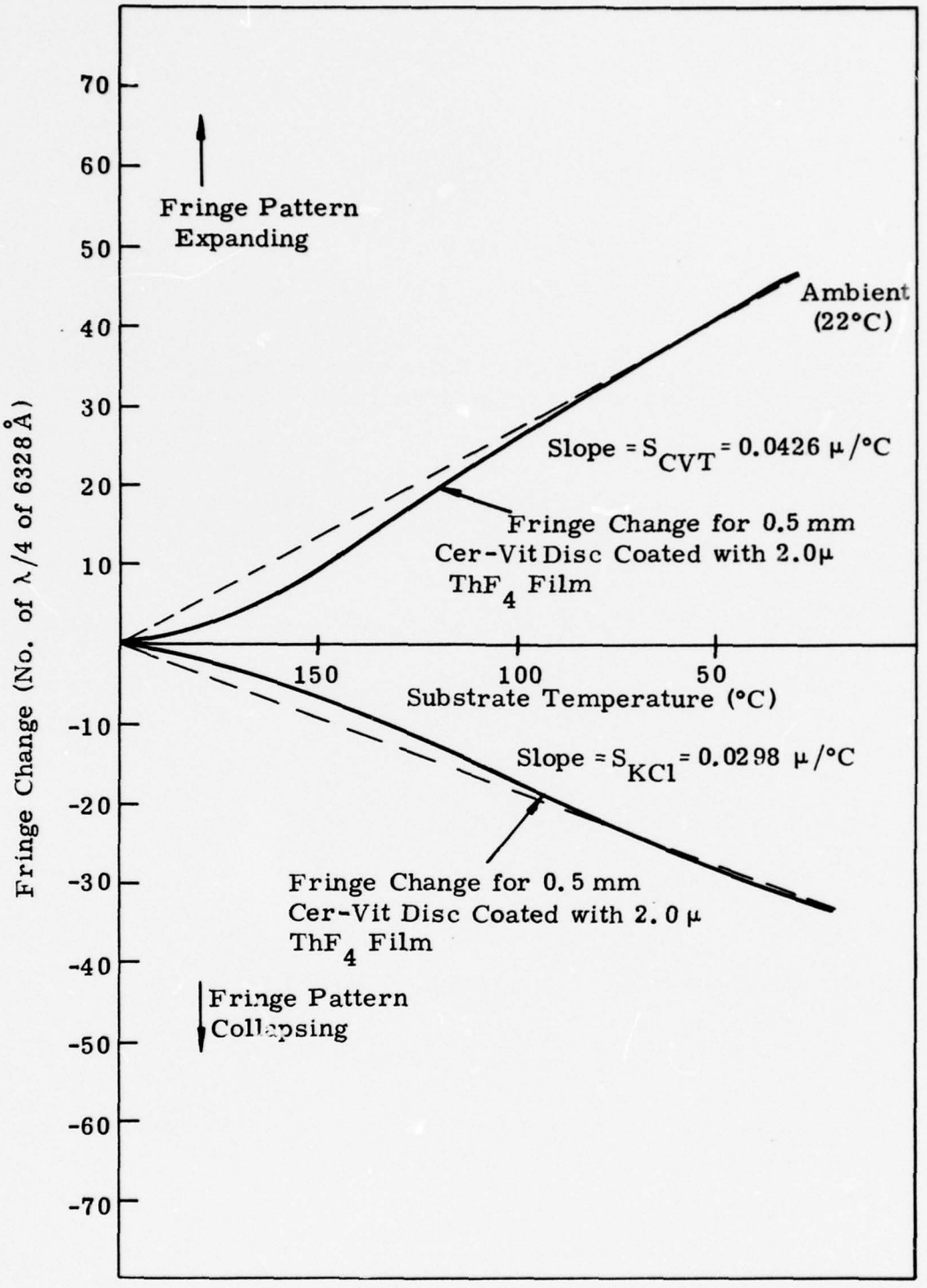

Figure 14. Thermally Induced Fringe Changes for Cer-Vit and KCl Substrates Coated With ThF_4

If two different substrate materials are coated with identical films, the deflections are correspondingly

$$\omega_1 = \frac{3(1 - \nu_1)\, t}{4E_1} \left(\frac{D_1}{h_1}\right)^2 E_f \quad (\alpha_f - \alpha_1)\, \Delta T$$

and

$$\omega_2 = \frac{3(1 - \nu_2)\, t}{4E_2} \left(\frac{D_2}{h_2}\right)^2 E_f \quad (\alpha_f - \alpha_2)\, \Delta T$$

Here, ω_1 and ω_2 are the total deflections of the disc that occur between two ambient temperatures operated by a temperature ΔT.

Letting

$$\Lambda_1 = \frac{3(1 - \nu_1)}{4E_1} \left(\frac{D_1}{h_1}\right)^2 \text{ and } \Lambda_2 = \frac{3(1 - \nu_2)}{4E_2} \left(\frac{D_2}{h_2}\right)^2$$

and writing the slope of the curves in Figure 13 as

$$S_1 = \omega_1/\Delta T$$

$$S_2 = \omega_2/\Delta T$$

The thin-film expansion coefficient is derived as

$$\alpha_f = \frac{\alpha_2 S_1 \Lambda_2 - \alpha_1 S_2 \Lambda_1}{(S_1 \Lambda_2 - S_2 \Lambda_1)}$$

and Young's modulus of elasticity is given by

$$E_f = \frac{S_2}{\Lambda_2} \quad \frac{1}{(\alpha_f - \alpha_2)\, t} \quad \text{kg/cm}^2$$

The deflections shown in Figure 14 give the following values for these two material properties for ThF_4 deposited at 200°C:

$$\alpha_f = 18.6 \times 10^{-6}/°C$$

$$E_f = 6.9 \times 10^5 \text{ kg/cm}^2$$

Since the expansion coefficient lies between that of Cer-Vit ($2 \times 10^{-8}/°C$) and that of KCl ($36 \times 10^{-6}/°C$), the thermally induced stresses in the coating are in the opposite direction, and the intrinsic stress of the ThF_4 film on KCl becomes compressive whereas greatly increased tensile

stress is developed for the ThF_4/Cer-Vit sample. The entire stress history from deposition through cooldown in vacuum is shown in Figure 15, where the thermally induced stress is approximately twice the intrinsic stress and is sufficient to produce a final compressive stress of 1400 kg/cm^2 on KCl and a large tensile stress of 3400 kg/cm^2 when ThF_4 is deposited onto Cer-Vit. A knowledge of these two stress contributions is fundamental to any stress addition model and can now be conveniently measured using the stress-interferometer system.

2.8 SUMMARY OF INTRINSIC AND THERMAL STRESS MEASUREMENTS FOR ThF_4 FILMS

A system of stress-measuring interferometers has been fabricated and has been used to characterize the stress properties of thick films of thorium fluoride. Interferometric system characteristics provide the following:

- Stable, vibration-insensitive operation of a system of four cat's-eye interferometers together with a sampled data acquisition system and data reduction codes is complete.

- Stress measurements can be made in vacuum at high temperature (250°C) on 4 different substrate materials at 4 different vapor-incidence angles. The stress behavior of combinations of thin-film materials can be obtained by the use of remote shutters.

- The interferometer system can measure both intrinsic stress produced during deposition together with thermally induced stress caused by temperature changes.

The stress properties of single films of thorium fluoride have been measured to check some basic assumptions used in the measurement system. These experiments show that:

- The measured stress is independent of the thickness of the flexible substrate utilized in the interferometer for disc thicknesses in the range 0.25 to 1.0mm.

- The measurement of intrinsic stress in identical films deposited onto different substrate materials shows that the type of substrate does not significantly influence stress measurements and that the largest errors can occur from errors in the values assumed for the elastic constants of the plate (Young's modulus and Poisson's ratio).

Experimental measurements for thorium fluoride films under a variety of deposition conditions indicate the following:

- Intrinsic stress levels for thick films of thorium fluoride using Cer-Vit and fused silica discs show little dependence upon vapor incidence angles in the 0.0 to 40 degree range.

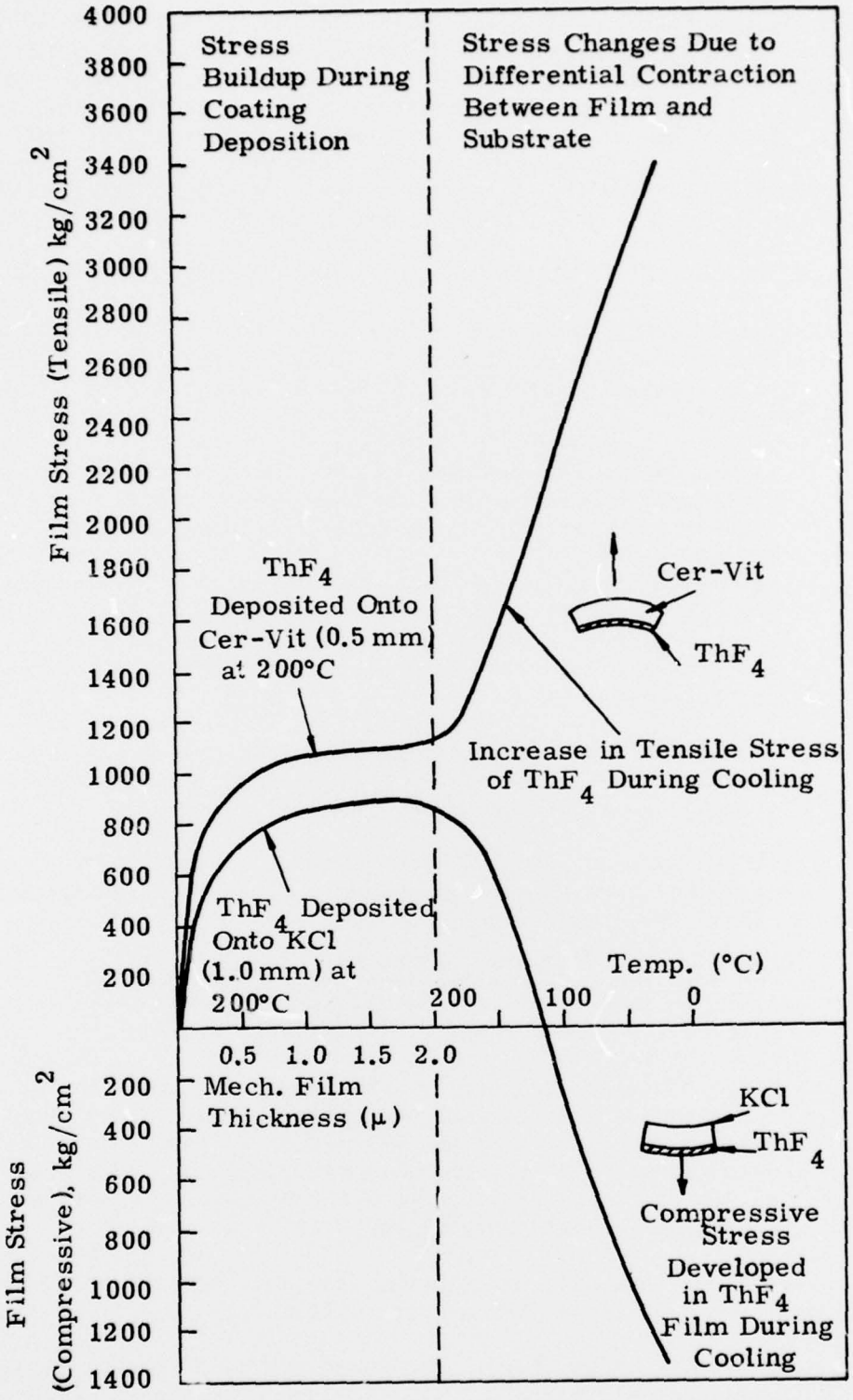

Figure 15. Intrinsic and Thermally Induced Stresses in ThF4 Films Deposited Onto Cer-Vit and KCl Substrates at 200°C

- Equilibrium stress levels for thick films of ThF_4 are relatively independent of temperature and rate of evaporation. Slightly larger equilibrium occurs for lower temperatures and for low evaporation rates, but the differences are only 10 to 20% of the final average stress value.

- A comparison of the present stress measurements compared with those of Ennos[2] for thorium oxyfluoride show similar characteristics up to 0.5 micron thickness, i.e., a rapid rise in stress for low evaporation rates and an equilibrium stress of 1500 kg/cm^2 for ambient-temperature deposition (curve shown dotted in Figure 13).

Stress changes in thorium fluoride films due to thermally induced deflections show that:

- The stress in ThF_4 deposited onto KCl substrates is initially tensile (~ 1100 kg/cm^2), but differential thermal contraction during cooldown produces a net compressive stress (1400 kg/cm^2) at room temperature. A corresponding tensile stress increase from 1100 kg/cm^2 to 3400 kg/cm^2 is produced when ThF_4 is deposited onto Cer-Vit substrates.

- Measurement of the deflection of different material/film combinations during cooldown can provide values of the thermal expansion coefficient (α_f) and Young's modulus (E_f) of the thin-film material. Our preliminary results show that for ThF_4 (200°C deposition)

$$\alpha_f = 18.6 \times 10^{-6}/°C$$

$$E_f = 6.9 \text{ kg/cm}^2$$

Investigation of high index materials such as zinc selenide and/or thallium iodide will be conducted during the remainder of the program in single-film form and in combination with a low index material such as thorium fluoride, potassium chloride or sodium fluoride. Such materials are used to antireflect KCl windows and can provide low absorption for coatings in the 10.6 micron region.

The theoretical work performed during the program to establish models for the addition of stresses in multilayer film on high expansion substrates is described in Section 3. This effort is aimed at relating the physical breakdown of such film systems to their internal stress levels under changing temperature conditions. The treatment of film stresses is macroscopic at present since the nucleation phase of film growth during the first several hundred Angstroms is a small part of the total thickness of films for infrared applications.

SECTION 3

COMPUTER MODELLING OF STRESS ADDITION IN MULTILAYER THIN-FILM COATINGS

The goal of this phase of the program is to develop computer codes to enable the stress levels in multilayer stacks to be predicted as a function of temperature. Changes in temperature can be caused by environmental changes or by laser beam heating, and both sources can lead to film fracture and delamination. The overall aim of such a computer model is to enable the thin-film designer to predict stress levels in antireflection coatings and in particular, to predict thermally induced failure levels when the substrate material has a high thermal expansion coefficient, as in the case of KCl.

As a starting point for this discussion, we derive the deflection due to stress in a thin circular plate resulting from the addition of a single stressed film on its surface and include stress relief effects and the effect of changes in ambient temperature.

3.1 DEFLECTION OF A CIRCULAR PLATE DUE TO THIN-FILM STRESS

Although the equation for the deflection of a thin disc due to a stressed coating has been derived by many authors, we include the derivation here for the sake of clarity. The equation for stress and deflection derived in the following discussion assumes that:

(1) The film properties are uniform, i.e., unit stress is independent of film thickness.

(2) The disc is stress-free and no twisting moments exist within the material or are induced in the disc by the deposition of a thin film of material (i.e., stress is isotropic).

(3) Deflections are small compared with the substrate thickness.

(4) No slippage occurs at the film substrate boundary.

If the circular plate has a thickness h and a diameter D, the initially unstressed disc is bent to a sphere by the film and the neutral surface of the disc assumes a sphericity γ, as shown in Figure 16a. The film shown in Figure 16a is under tensile stress, and the deflection (w) of the neutral surface due to the film stress is for small deflections.

$$w = \frac{D^2}{8r} \qquad (1)$$

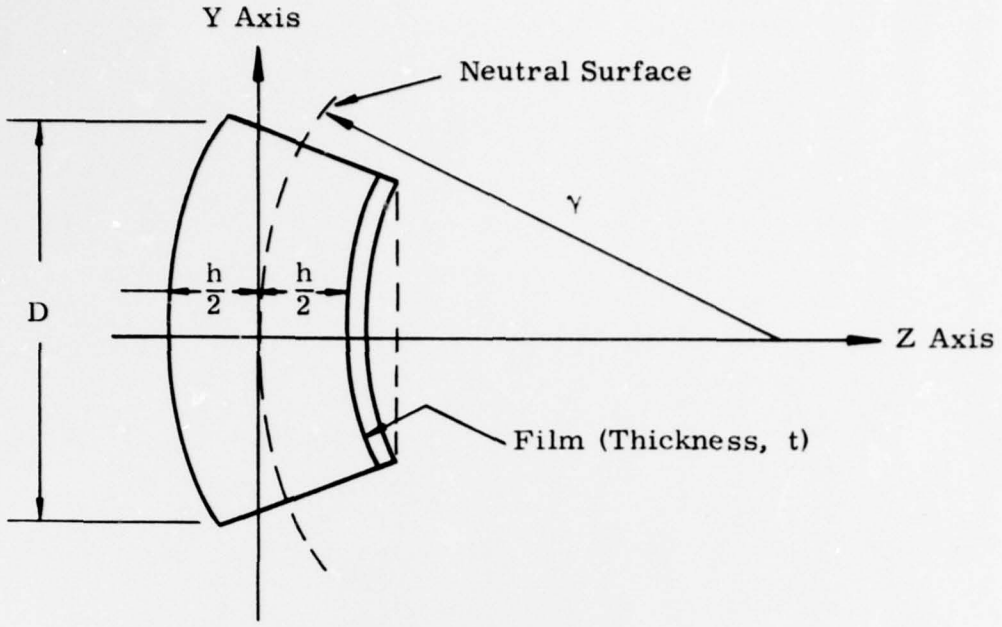

Figure 16a. Deflection of Disc Due to a Single Film

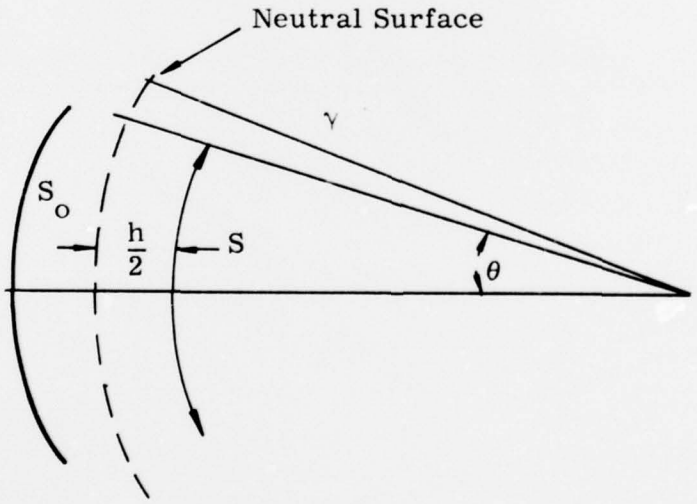

Figure 16b. Stress Relief Effects

The bending moment M and the disc radius (r) are related by[12]

$$\frac{1}{r} = \frac{M}{A(1+\upsilon)} \tag{2}$$

where

$$A = \frac{Eh^3}{12(1-\upsilon^2)} \tag{3}$$

and

$$M = \int_{h/2}^{h/2+t} \sigma z dz \tag{4}$$

Here the material parameters are

E = Young's modulus of elasticity

υ = Poisson's ratio

σ = Unit stress in the film (i.e., stress in a thin layer dz at d distance z from the neutral surface)

Combining Eq. 1, 2, and 3, the deflection (w) in terms of the induced bending moment (M) becomes

$$w = \frac{3}{2} \frac{(1-\upsilon)}{E} \left(\frac{D^2}{h^3}\right) M \tag{5}$$

If, as is usually assumed (although definitely not the case for real films), the unit stress is independent of Eq.3, the bending moment is simply

$$M = \sigma \int_{n/2}^{h/2+t} z dz = \frac{\sigma h t}{2} \left(1 + \frac{t}{h}\right)$$

If the mechanical film thickness $t \ll h$ (the plate thickness), a further simplification gives

$$M = \frac{\sigma h t}{2} \tag{6}$$

and the deflection from Eq. 5 is now written as

$$w = \frac{3}{4} \left(\frac{1-\upsilon}{E}\right) \left(\frac{D}{h}\right)^2 \sigma t. \tag{7}$$

Since the plate deflects during film deposition, a small amount of stress relief occurs. Alternately, if the external forces are applied to the plate such that the deflection (ω) is removed, the film is stretched (i.e., subjected to tensile forces), and the true film stress is larger than if the plate is allowed to bend freely.

In Figure 16b, the unit elongation (ϵ) is given by

$$\epsilon = \frac{s_o - s}{s} = \frac{\gamma\theta(\gamma - h/2)\theta}{(\gamma - h/2)} = \left(\frac{h}{2\gamma - h}\right)$$

Again, assuming $h \ll \gamma$, the unit elongation is

$$\epsilon \doteq \frac{h}{2\gamma}$$

and in terms of the plate deflection (Eq. 1)

$$\epsilon = \frac{h}{2} \cdot \frac{8\omega}{D^2}$$

resulting in a stress

$$\sigma_\gamma = \frac{E_f h 4\omega}{D^2}$$

where E_f is the Young's modulus for the thin-film material.

The total film stress including stress-relief is thus

$$\sigma_{Total} = \left(\frac{\omega}{t}\right)\left(\frac{4}{3}\right)\left(\frac{E_s}{1-\upsilon}\right)\left(\frac{h}{D}\right)^2 + \frac{4E_f h\omega}{D^2} \qquad (8)$$

$$\sigma_{Total} = \left(\frac{\omega}{t}\right)\left(\frac{4}{3}\right)\left(\frac{E_s}{1-\upsilon}\right)\left(\frac{h}{D}\right)^2 \left\{1 + 3(1-\upsilon)\left(\frac{E_f}{E_s}\right)\left(\frac{t}{h}\right)\right\} \qquad (9)$$

The correction term can be seen to be small involving the ratio t/h, assuming that the Young's moduli for the film (E_f) and substrate (E_s) are of comparable size.

3.2 TEMPERATURE-INDUCED STRESS CHANGES

Thin films are usually deposited onto hot substrates to improve adhesion and durability and to reduce optical absorption in the 10-micron region. The temperature changes occurring for a film/substrate combination induce changes in stress in the film due to differential thermal expansion between the two

materials. This effect is readily seen in the stress-measuring interferometer system, where deflections of the substrate are caused by

(1) The heating cycle

(2) Evaporation source temperature changes

(3) Movement of hot shutters under the substrate

(4) Cooldown to ambient temperature changes

Additional stress-relief can also be caused when the system is vented to air. The temperature-induced stress changes in the film can be determined accurately from the deflections of the stress interferometer and can be used to estimate the values of Young's modulus and thermal expansion coefficient of a single thin-film material. These constants are usually not known for material in thin-film form, and bulk values are usually substituted for calculation purposes. The stress induced by a temperature change ΔT is calculated as follows for a thin-film substrate sample.

The unit elongation of an element of the film is simply

$$\epsilon_f = \alpha_f \Delta T$$

where α_f is the thermal coefficient of expansion of the film material. Similarly, the unit elongation of the substrate is

$$\epsilon_s = \alpha_s \Delta T$$

Since the film adheres to the substrate, it cannot physically elongate more than the substrate elongates; hence, the ex ess elongation of the film $(\epsilon_f - \epsilon_s)$ can only be prevented by the presence of a compressive stress

$$\sigma_f = E_f \epsilon = E_f (\epsilon_f - \epsilon_s) \Delta T \qquad (10)$$

The preceding equations for the total stress and stress-relief in a thin dielectric film assume that the instantaneous stress is constant within the deposited film. Experimental results given here and by Ennos and others show that the average measured stress $< S >$ changes during film growth and, consequently, the instantaneous or unit stress σ (t) is thickness dependent. The relationship between the experimentaly measured stress $< S >$ and the instantaneous stress σ (t) is obtained by considering the origin of the bending moment (M) , which produces deflection of the disc. The integrated bending moment due to a film of thickness t at a distance h/2 from the neutral surface produces a deflection that is equivalent to the existence of an average stress $< S >$ in a film of thickness t at a distance h/2 from the neutral surface; i.e.,

$$M = \int_{o}^{t} \sigma\,(t)\;(h/2 + t)\;dt = h/2 < S > + \qquad (11)$$

The unit stress can therefore be obtained from the measured data as

$$\sigma\,(t) = \left(\frac{h/2}{h/2+t}\right)\;\frac{d}{dr} < S > t$$

which, for $t \ll h/2$, reduces to

$$\sigma\,(t) = < S > + t\;\frac{d < S >}{dt} \qquad (12)$$

In practice, the stress data $< S >$ can be approximated by a polynomial expression in terms of film-thickness, i.e.,

$$< S > = \sum_{k=o}^{\infty} a_k t^k \qquad (13)$$

where the coefficients a_k are obtained using a least-squares best fit to the experimental sampled data.

3.3 STRESS ADDITION IN MULTILAYER FILMS

If several films are deposited onto a flexible glass substrate of thickness h and if each film has a thickness (t_i) and a thickness-dependent stress $\sigma_i(z)$, the bending moment generated is given by

$$M = \int_{h/2}^{h/2 + t_1} \sigma_1(z)zdz + \int_{h/2 + t_1}^{h/2 + t_1 + t_2} \sigma_2(z)zdz + \int_{h/2 + t_1 + t_2}^{h/2 + t_1 + t_2 + t_2} \sigma_3(z)zdz + - - -$$

or for a total of m films

$$M = \sum_{k=1}^{m} \int_{h/2 + \sum_{j=1}^{k-1} t_j}^{h/2 + \sum_{j=1}^{k} t_j} \sigma_k(z)zdz \;\; --- \qquad (14)$$

The thickness dependence of the stresses measured for thorium fluoride during the present study show a dependence of the form

$$< S > = S_o\;(1-at)\;(1-e^{-bt}) \qquad (15)$$

and it is tempting to fit stress curves to this functional form. However, the stress data is generally a polunomial expression that will be obtained as a least-squares best fit to the experimental data.

If the stresses $\sigma_i(z)$ are assumed constant, Eq. 14 can be integrated to give

$$M = \sum_{k=1}^{m} \sigma_k \left\{ \frac{t_k \left(h + 2 \sum_{j=1}^{k-1} t_j\right) + t_k^2}{2} \right\} \qquad (16)$$

and for small values of ϵ, one simply obtains the bending moment as

$$M = \frac{h}{2} \sum_{k=1}^{m} \sigma_k t_k \qquad (t \ll h)$$

and the deflection of the substrate as

$$\omega = \left(\frac{3}{4}\right) \frac{(1-\nu)}{E_s} \left(\frac{D}{h}\right)^2 \sum_{k=1}^{m} \sigma_k t_k \qquad (17)$$

The thickness-dependent stresses can be measured experimentally for each film in a multilayer during deposition, and the stress changes due to temperature changes can be measured after the entire film system is fabricated. Taking the simplest case of a multilayer coating (i.e., a three-layer antireflection coating of KCl), the present interferometer system allows the three individual layers to be deposited onto three different substrates and the entire multilayer to be deposited onto the fourth substrate during the same evaporation run. This type of experiment is illustrated schematically in Figure 17.

The first step, therefore, in developing a theory of intrinsic and temperature-induced stresses in thin-films is to develop a computer model that enables the deflection of a flexible substrate to be calculated for a multilayer in terms of the individual measured instantaneous stresses $\sigma_i(t)$ and then to predict the deflection changes with temperature. A knowledge of the stress buildup is only of use if the breaking stresses of the individual thin-film materials are known since only in this way can one predict the durability of thin-film systems to temperature changes.

The breaking stress can be determined by depositing identical films onto rigid and flexible substrates and measuring the stress (on the flexible substrate) at which the film on the rigid substrate begins to crack. The measurement technique to determine the film rupture point on the rigid substrate has not yet been fully developed, but a preliminary method will detect the increase in scatter of a He-Ne laser beam after two passes through the depositing film. An alternative method is to view the film through a microscope while the film is being heated although this presupposes that the film will not rupture during the deposition on the cool-down cycle during fabrication.

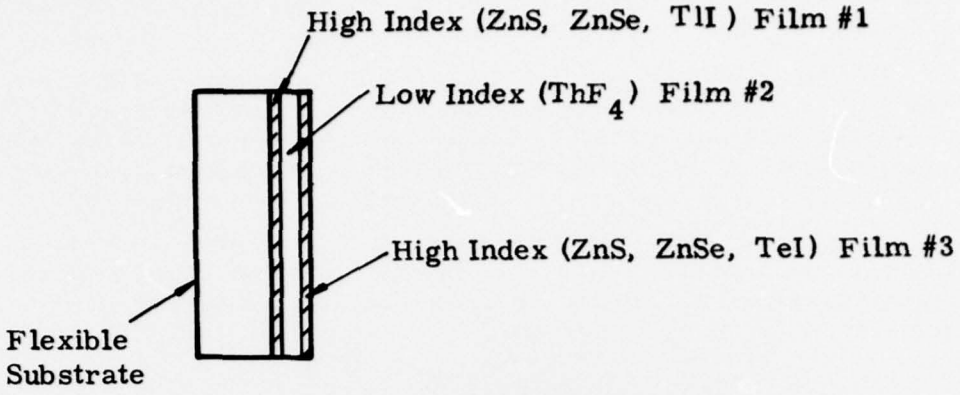

Interferometric Stress-Measurement Arrangement

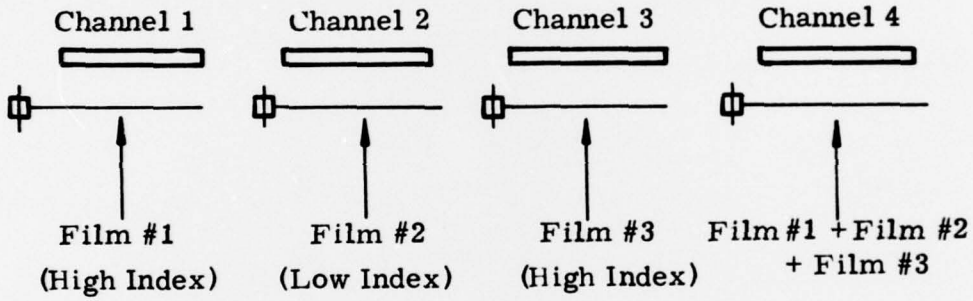

Stress Addition (Dotted Lines Show Effect of Temperature Changes)

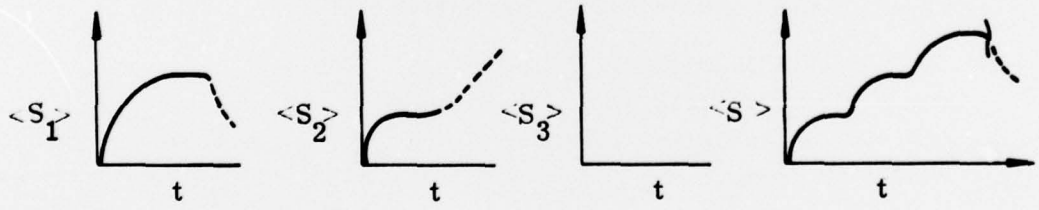

Figure 17. Stress Addition in Antireflection Coatings

3.4 COMPUTER MODEL FOR INTRINSIC AND THERMALLY INDUCED STRESSES IN MULTILAYERS

The computer model will attempt to describe the deflections obtained for a thin flexible disc when a multilayer dielectric stack of films is deposited onto the surface. The stress of individual films is determined experimentally, and the effect of temperature changes must also be explained.

The total deflection of the plate (ω_{TOT}) is caused by the addition of bending moments caused by stress in the deposited films together with temperature-induced bimetallic effect and stress-relief effect. The total deflection can be expressed as

$$\omega_{TOT} = \left(\frac{D}{h}\right)^2 \frac{3}{2}\left(\frac{1-\nu}{E_s h}\right) \sum_{k=1}^{m} \int_{h/2 + \sum_{j=1}^{k-1} t_j}^{h/2 + \sum_{j=1}^{k} t_j} \left\{\sigma_k(z) + E_k(\alpha_k - \alpha_s)\Delta T\right\} z\,dz \qquad (18)$$

and the deflection can be separated into the intrinsic stress term obtained from the measured values of unit stress $\sigma_k(z)$ for the individual films at constant temperature together with a thermally induced stress produced during the cooldown cycle; i.e.,

$$\omega_{TOT} = \left(\frac{D}{h}\right)^2 \frac{3}{2}\left(\frac{1-\nu}{E_s h}\right)\left[\sum_{k=1}^{m} \int_{h/2 + \sum_{j=1}^{k-1} t_j}^{h/2 + \sum_{j=1}^{k} t_j} \sigma_k(z) z\,dz + \sum_{k=1}^{m} E_k(\alpha_k - \alpha_s)\Delta T \left(\frac{h}{2}\right) t_k\right] \qquad (19)$$

The amount of stress-relief for the entire film stack can also be calculated from the total deflection (ω_{TOT}) as shown in Section 3.1. Eq. 19 provides the basis for the stress-addition model, although the presence of additional factors such as transient heating due to opening and closing of shutters below each substrate can also be included.

3.5 SUMMARY OF STRESS-ADDITION MODELS

The addition of stresses in thin-film multilayers has been formulated on a macroscopic basis and requires the following experimental data for each deposited film in order to predict the resultant stress in multilayers.

- The variation of unit stress with deposited film thickness. (This function is derived from the stress measured during film deposition.)
- The effective values of Young's modulus of elasticity and thermal coefficient of expansion obtained from thermally induced stresses produced after film deposition.

Experimental data of this form has been obtained for thorium fluoride films, and similar measurements for other materials will constitute the input data to the computer model.

SECTION 4

WORK SCHEDULED FOR REMAINDER OF PROGRAM

The program effort until the end of the conract will be directed towards the following tasks.

- Experimental determination of unit stress and thin-film constants (E_f and α_f) for zinc selenide and thallium iodide for use as the high-index material in antireflection coatings for KCl.
- Experimental determination of intrinsic and thermally induced stresses in the component films and the entire film stack of a 2 or 3 layer antireflection coating.
- Measurement of thin-film absorption data for the component materials of the antireflection coating using laser calorimetry.
- Development and implementation of a computer program to calculate the resultant stress in multilayer coatings during heating.
- Determination of the breaking stresses of thin-film materials deposited onto rigid substrates.
- Verification of the stress addition model.
- Verification of the film rupture model due to thermally induced stresses resulting from temperature cycling or laser beam heating.

SECTION 5

REFERENCES

1. E. Crittenden and R.W. Hoffman, Phys. Rev. 78, 349 (1950).
2. A. E. Ennos, Appl. Optics, 5, 1, p51 (January 1966).
3. J.D. Wilcox and D.S. Campbell, Thin Solid Films, 3, 3 (1969)
4. H.S. Story and R.W. Hoffman, Proc. Phy. Soc. (London), B70, 950 (1957).
5. J.S. Halliday, T.B. Rymer, and K.H.R. Wright, Proc. Roy. Soc. (London), A225, 548 (1954).
6. A. Kinnabara and H. Harabi, J. Appl. Phys. (Japan), 4, 243 (1965).
7. R.W. Hoffman, Phys. of Thin Films, 3, 211 (1966).
8. K. Kinosita, Thin Solid Films, 12, 17 (1972).
9. R.W. Hoffman, Thin Solid Films, 34, 185 (1976).
10. R. Carpenter and D.S. Campbell, J. Matl. Science, 2, 173 (1967)
11. J.R. Kurdock and E.A. Strouse, "Optical Processing of Alkali Halides and Polycrystalline Zinc Selenide for High Power Laser Applications", AFML-TR-74-166, Part II, Contract No. F33615-73-C-5127 (July 1975).
12. S. Timoshenko, Theory of Plates and Shells (McGraw-Hill, New York, 1959), 2nd ed., p.43.